5-2013

Miscibility and influence on each other of a UV photo-initiated thermosetting polymer blend of radical and cationic systems

Kevin Lefebvre
University of Nebraska-Lincoln, kev.lefebvre@yahoo.com

Miscibility and influence on each other of a UV photo-initiated thermosetting polymer blend of radical and cationic systems

By

Kevin Lefebvre

A THESIS

Presented to the Faculty of

The Graduate College at the University of Nebraska

In Partial Fulfillment of the Requirements

For the Degree of Master of Science

Major: Mechanical Engineering and Applied Mechanics

Under the Supervision of Professor Li Tan

Lincoln, Nebraska

May, 2013

Miscibility and influence on each other of a UV photo-initiated thermosetting polymer blend of radical and cationic systems

Kevin Lefebvre, M.S

University of Nebraska, 2013

Adviser: Li Tan

Thermoset blends engage an interest into polymer materials using photopolymerization. Our work is inscribed within a project which consists to control the degree of crosslinking in three dimensions during UV photo-curing. Two different reaction mechanisms were considered to enlarge the control of properties. The goal of this thesis was to check the miscibility between two thermosetting polymers using radical and cationic chemical mechanisms. Then their influence on each other was studied by thermal analysis. The experimental system was Bisphenol A propoxylate diacrylate for the radical curing and 3,4-epoxycyclohexylmethyl 3,4-cyclohexanecarboxylate for the cationic. They were initiated by 2-hydroxy-2-methylpropiophenone and Triarylsulfonium hexafluoroantimonate salts mixed respectively. Several polymer blends were manufactured and influence of weight proportions and process temperature were studied. As a result, high thermal stability and properties were determined and homogeneity of these materials was verified by Thermogravimetric Analysis. Differential Scanning Calorimetry showed that thermal properties of blended materials didn't follow any linear blending law. It was also noticed that the temperature needs to be highly considered. The cationic resin, which used to be post-cured to reach a high degree of curing, was highly cured at 80°C. But the radical network, which used to crosslink very fast at ambient temperature, didn't fully cure. We concluded that some interactions occur between the two systems but the presence of Interpenetrating Polymer Networks was not confirmed.

Acknowledgments

I would like to thank everyone who helped me and shared my life during my master's degree. My first personal acknowledgment goes to Dr. Tan. Li, there is no word to express you all my thankfulness, gratitude and respect. Even though we sometimes had a hard time to get along together, I truly appreciated your advices and your way to share your experience. Thank you for helping me to find myself and get more self-confident. Dr. Negahban, thank you for your directions, your help and your reassurance all along my experience in your department. Dr. Saiter, I can never thank you enough for allowing and pushing me to take part of this program. This amazing experience made me more open-minded and grown up. To Dr. Delpouve, thank you so much for your managing, your patience and sharing your passion. Your directions helped me to be more organized and enjoy my work better. Thank you to Dr. Youssef for his help, his support and his friendship. I want to express my combined acknowledgment to Dr. Saiter and Dr. Negahban, thank you for giving so much of yourselves to push this unique experience forward.

It was a great pleasure to work with Dr Tan's research group. These teammates were very easy to get along with. It was a pleasure to share their knowledge in a relaxed and friendly atmosphere. I would like to particularly thank Dr Jiang for helping and teaching me with chemistry. This domain was very difficult and scary to work on before. Jinyue, thank you for sharing your lab, your passion and your professionalism, as a teammate and as a friend.

To my family and friends from France, you have always been on my side and being so far away from each other just got us closer. This experience was a real accomplishment for me and you know how important it was for me to make it. Thank you for being understanding and supportive.

To the people I met in Lincoln, NE, thank you for making my American life what I was. Wherever you come from, you contributed to make me experiment your way of life and your culture. I made really good friends from you. I am so grateful to you since you made me love your country and feel like to come back. Thank you to Séverine for welcoming me and introducing me to my social, scholar and professional life in the United States of America.

This thesis was made possible by the collaboration between the University of Nebraska-Lincoln and the University of Rouen.

Contents

List of figures

List of tables

Chapter 1

Introduction

Thermosetting polymers are light materials able to provide properties comparable to those of some metal alloys. They are one of the three general families of polymers. Elastomers are polymer materials with a very low glass transition temperature and huge elongation strains. They are used to be called rubbers and are made of long polymer chains with a very low degree of crosslinking. Thermoplastics are another type of polymer. Their long molecular chains and their intermolecular interactions allow them to be moldable above a specific temperature called glass transition (Tg). Some of them can be partially crystallized though.

Despite being plastics, thermosets can have high heat resistance, chemical resistance and important mechanical properties. They are also known as thermosets. They have a particular interest in this subject. Unlike thermoplastics, these materials have an irreversible cure realized for example using heat, electron beam or light. Initially, they are used to be liquid or malleable and then cured into their final form. A 3D network is created during the reaction with a crosslinking degree much higher than elastomers. This leads to a high glass transition material with a thermal stability stronger than thermoplastics.

Nowadays, the increasing demand of specific requirements for industrial applications leads towards the creation of new materials. There are different ways properly used to design polymer materials. New molecules can be imagined and synthetized in order to reach some expected properties. We can use polymers already existing and combine them together to get better, average or antagonist properties compared to those of separate components. These properties depend a lot on the process used to mix the polymers and cure the final material. For example, compounds can be stirred in a liquid state or mixed into a reactive extruder if they are more viscous.

In a lot of cases, polymer chains don't mix very well and form phase separation leading to the loss of the expected properties at microscopic or macroscopic scale. Poor adhesion between phases is origins of phase separation. To avoid the issue of incompatibility, special agents like surfactants are usually added to increase their miscibility or polymers are chemically modified. Then, we can end up with materials having homogeneous, uniform and controlled properties. Depending on the processing strategy, they will be either called copolymers or blends. A copolymer is a polymer which the chain is made of at least two monomeric species [1]. It is homogeneous at the molecular scale i.e. all the chains are similar. There are different sort of copolymer arrangements (Figure 1) depending on the monomer species and the polymerization process. For example, the most common ones are statistic copolymers, in which both components have a random arrangement on the final chain. These materials finally have intermediate properties between those of which separate homopolymers. Synergic interactions can also be expected. Polymer blends are formed from two or more polymer

chains blended together. These chains can be miscible; then the material will have one glass transition and a single-phase structure. Or they can be immiscible; in that case, many glass transitions will be observed. If interactions between component chains are not strong enough, phase separation will occur. A usual way of mixing them together is to use an extruder [2].

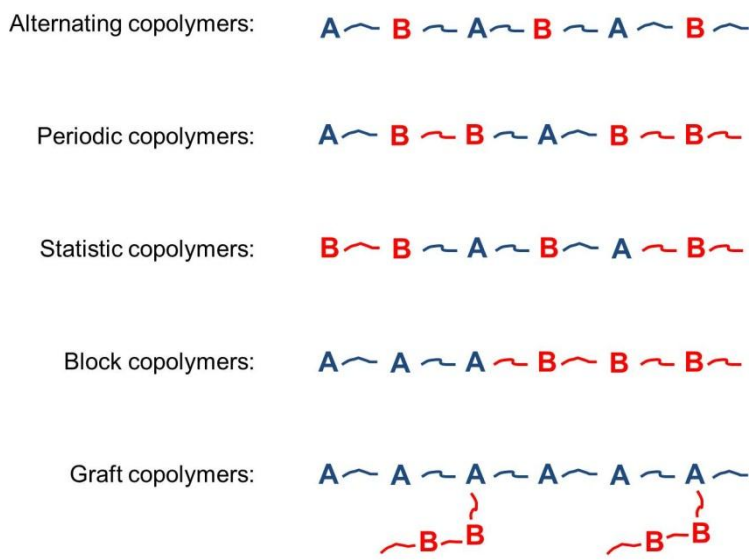

Figure 1: Representation of different molecular chains of copolymers made from monomer species A and B

Today, the creation of blends or copolymers is highly developed in the field of polymer chemistry research. If these two systems differ by their chemistry, it is important to notice that they both aim leading to specific homogeneous properties.

Regular polymer blends usually ends up to a compromise between separate properties. Martin et al. [3] blended polymers with opposite properties. Actually, they mixed a rubbery material and a glassy one. In this kind of studies, the first step is to

check the state of miscibility between the two components, using for example Dynamic Mechanical Spectroscopy in this cited case. Then presence of irregular interactions was determined by noticing non-linear modification of mechanical properties in function of components ratios.

In this work, we want to design a material by mixing two thermosetting networks. But we don't want any molecular interface within the material since it is well known in material science that interfaces can be origin of cracks and then decrease mechanical properties of the material. Our material may form an interpenetrating polymer network.

Interpenetrating polymer networks (IPN) are sometimes called as a special case of polymer blends [4, 5] but in fact an IPN is a polymer material containing two or more networks which are partially interlaced on a molecular scale but not on an atomic scale (Figure 2). That means there is no covalent bond between the networks but some irreversible entanglements are formed between them [6 - 10]. They are attracted together by weak interactions like Van der Waals. Once they are cured, the networks can't be separated from each other unless their own chemicals bonds are broken. A mixture of two or more performed polymer networks is not necessarily an IPN.

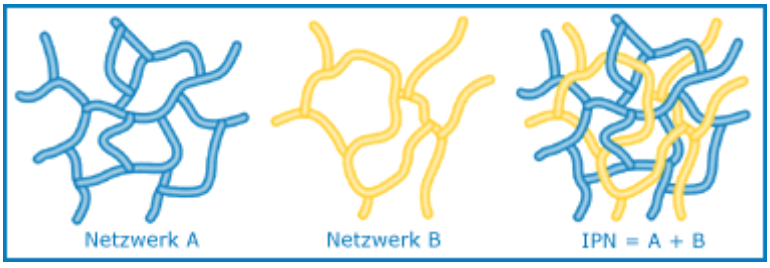

Figure 2: Representation of an Interpenetrating Polymer Network

To make an IPN, the involved polymer must be synthetized in presence of each other. At least one of them must be crosslinked to insure the cohesion of the network.

Akovali et al. [11] found an improvement of mechanical properties and resistance to solvents by mixing acrylonitrile and polystyrene into an IPN. Guo et al. [12] showed that mixing poly(ethylene glycol urethane) and unsaturated polyester resin in a gradient can end up to a synergic effect on mechanical properties of both materials. They also showed that the properties were not varying linearly with the components ratio. Tang et al. [13] demonstrated that gradient mixture of polyurethane and vinyl ester resin increased a lot the elongation at break compared to regular mixture. A clear improvement of mechanical and thermal properties is also revealed by gradients of interpenetrating polymer networks thanks to Lipatov et al. [14].

Our work is a contribution to a wider research project aiming at creating innovative gradient IPN. These materials are a particular case of IPN. Usually, IPN are classified depending on their process. If there are one crosslinked and one linear polymer, we talk about semi-IPN [6, 9]. The versatile aspect of the linear polymer finds applications for example in medical field. And we talk about full IPN if both polymers are crosslinked. In that case, the configuration is permanent. This kind of IPN is found in high mechanical properties applications. The Figure 3 helps to understand difference of arrangement between these two kinds of IPN.

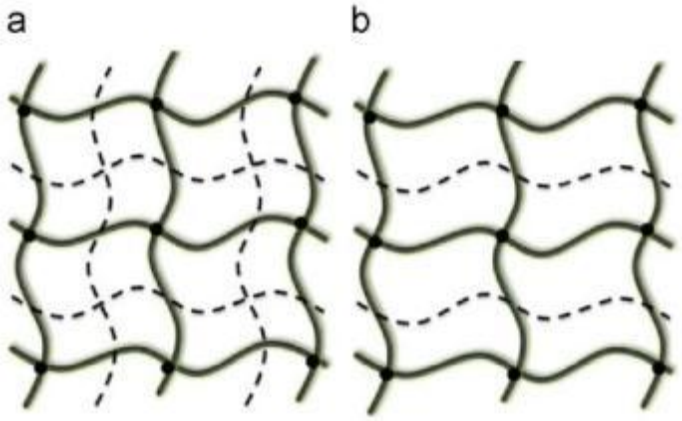

Figure 3: Scheme of a full IPN (a) and a semi-IPN (b) at the molecular scale (source: [8])

Many applications are found involving IPNs. A lot of them combine a rigid polymer and an elastomer to form tough plastics or reinforced elastomers depending on the proportions [15]. By being interpenetrated, each material solves its mechanical weakness using the mechanical strength of the associated polymer. Interpenetrating polymer networks can also solve problems of incompatibility from blends because they have lower interface interactions between the different components. Phase separation doesn't occur at the molecular scale anymore and the material appears uniform at a macroscopic scale. However, they may form finely divided phases of tens of nanometers. Studies showed that the size of these domains is smaller when the crosslinking rate is higher [9]. This means that many conditions need to be gathered in order to obtain an IPN. Kinetics and thermodynamics of each component must be matching to get the desired partial immiscibility. It is driven by equilibrium between phase separation and crosslinking rates. By example, if the separation phase rate is faster, the morphology of the IPN will be heterogeneous and the thermosetting networks will only partially interpenetrate [6]. These parameters are directed by experimental conditions, like initiators concentrations,

crosslinking density, temperature, or pressure. This can be defined by a phase diagram of the IPN [6, 9, 16].

IPNs are also classified according to kinetics. Concerned polymers can either be synthetized simultaneously, to properly form a simultaneous IPN. All the compounds must have a similar kinetic then. Photopolymerization is often used in order to have fast reactions at ambient temperature. Or a compound B can be swollen into a network A previously crosslinked. This ends up with what we call a sequential IPN [6]. It was reported by Gupta et al. [10] that sequential IPN are recognized for their greater thermal stability. Simultaneous synthesis can avoid problems of phase separation that occur with sequential IPN. They are often used for their improved mechanical properties compared to homopolymers.

Different ways lead to the creation of networks like thermal curing or electrons beam. Among them, UV-photo-curing get our interest because of its low energy consumption, its ambient temperature operation, the absence of solvent emission, the reduced reaction time and the high quality of the final product [17]. Furthermore, additional control of the reaction kinetic is given by temperature and light intensity. As shown on the Figure 4, temperature, which influences the bulk viscosity and so the molecular mobility and the diffusion, an increase of the light intensity and of the exposure time will increase the number of photons able to go through the matter [18, 19].

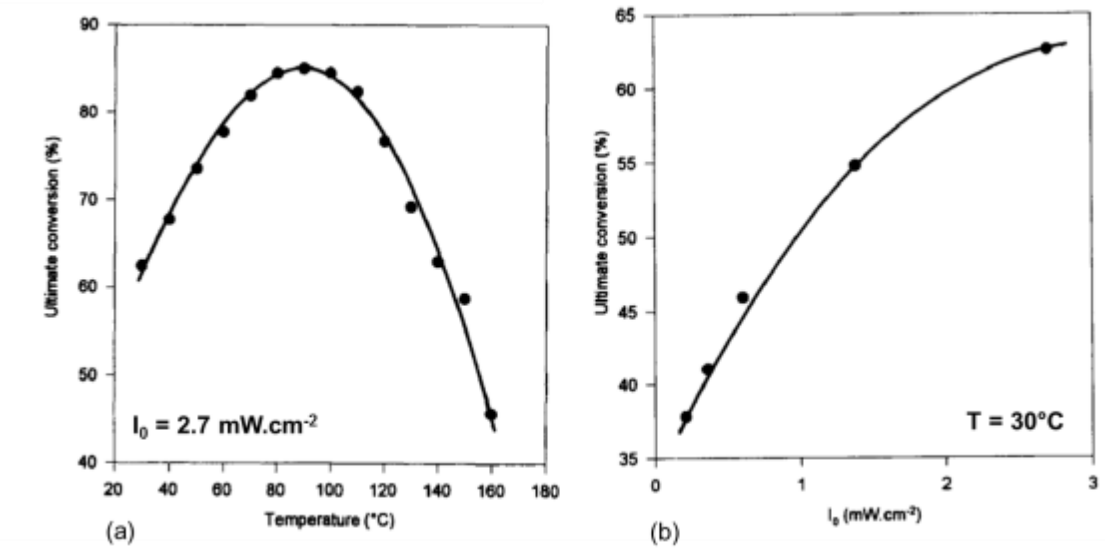

Figure 4: Influence of temperature (a) and light intensity (b) on the conversion of dimethacrylate oligomers [20]

To check the presence of Interpenetrating Polymer Networks, characterization technics like Thermogravimetric Analysis (TGA), Differential Scanning Calorimetry (DSC) or Dynamic Mechanical Analysis (DMA) are usually employed. Interpenetration is verified if the samples don't have a linear behavior in function of the compounds ratio, which is the signature of regular blends. For example, Simić et al. [7] showed that mixing Ethylhexyl Acrylate into acrylated hyperbranched Polyester doesn't lead to linear variation of mechanical properties. This phenomenon is observable on the Figure 5. This means that there exist some interactions between both components.

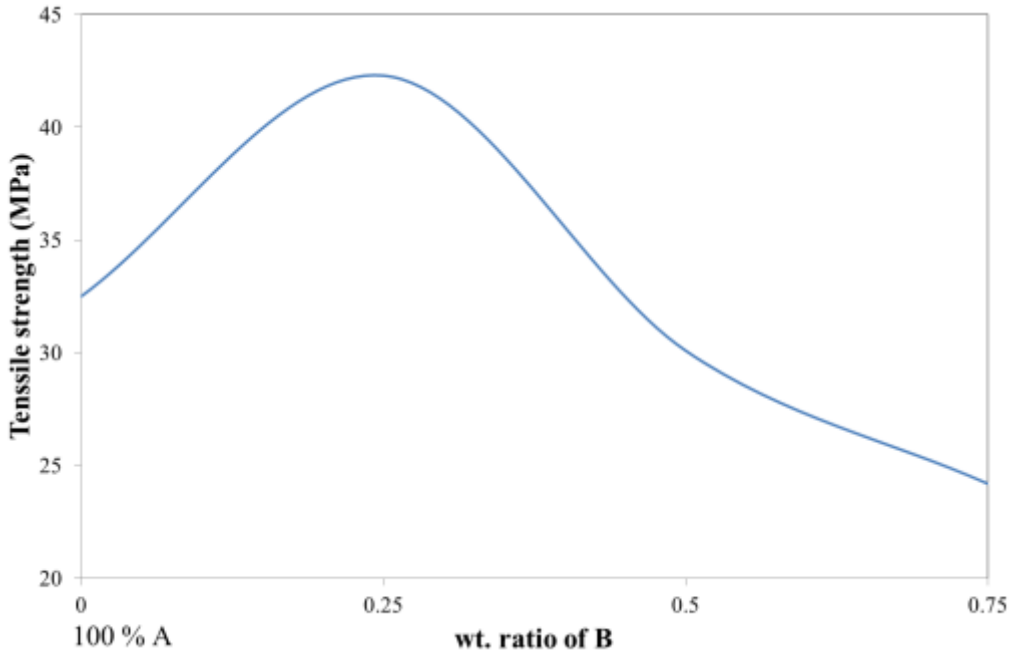

Figure 5: Influence of weight ratio of Ethylhexyl Acrylate into acrylated hyperbranched Polyester [7]

Using a single initiation mode usually ends up to a simultaneous IPN. For example, Tang et al. [13] used thermal curing to form their materials. Désilles et al. [16] preferred to use photo-curing for the first network and thermal curing for the second network to create a sequential IPN.

This study is dedicated to the UV-photo-curing of two thermosetting resins mixed at different compositions for investigating the possible existence of IPN. The chosen system is a blend of acrylate and epoxy crosslinkers curing respectively with a radical and cationic mechanism.

A photochemical reaction is directed by the absorption of an electromagnetic radiation with a wavelength λ. This radiation excites a reacting molecule called photo-

initiator. We use this extra component in the reaction because the crosslinker molecules are not sensitive to light and can't be initiated on their own. Photo-initiators are decomposed by absorbing the UV light and form radicals or ions able to initiate the chain reaction. They manage the first step of the photo-reaction and control the reaction rate.

To be efficient, a photo-initiator must have a high absorption in the emitting domain of the lamp. In order to transfer this energy, initiating molecules need an exact amount of energy to go to a higher level of energy, then, we say the molecule is excited. This is why these molecules are sensitive to some wavelength only. For a specific wavelength λ, energy carried by a photon is given by Planck law: $E = h.c/\lambda$

with h : Planck constant ($6{,}6261.10^{-34}$ J.s)

c : Light celerity ($2{,}9979.10^{8}$ m.s^{-1})

The Jablonski diagram can help to understand excitation mechanisms by radiation (Figure 6). When a molecule is in its initial state, its energy level is at its minimum ($^{1}A_{0}$), called fundamental state. Once a molecule is excited, it goes into an unstable excited state ($^{1}A^{*}$). Then the molecule comes back to its fundamental state by forming free radicals. It either releases this extra energy directly, this is called fluorescence. Or most of the time, It goes through an intermediate unstable state ($^{3}A^{*}$), which is still more stable than the excited state $^{1}A^{*}$. This is called phosphorescence. The reactive species are generated from this step.

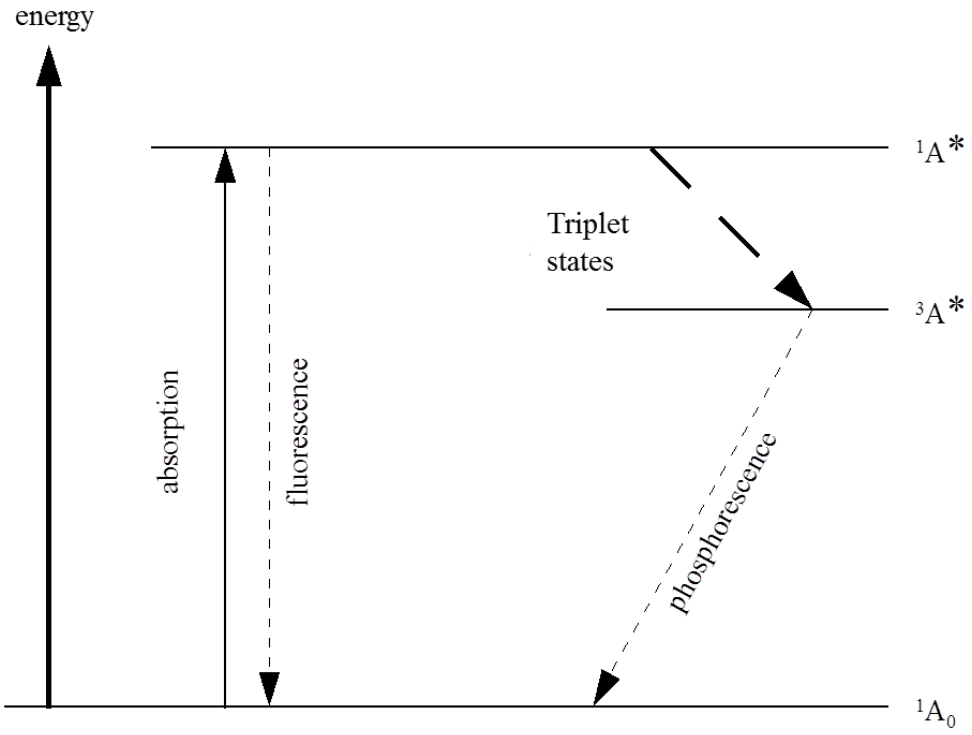

Figure 6: Schematic representation of an energy diagram (Jablonski diagram) showing the mechanism of fluorescence (source: Bioimaging©)

One of the focuses of this study is to investigate how the curing of a resin influences the curing of the other one in terms of kinetic, maximum conversion and resulting properties. The chosen crosslinkers cure respectively according to a radical and a cationic mechanism:

Radical reaction:

When the UV light hit the molecule, a cleavage between molecules occurs around the carbonyl group as shown on the Figure 7 [22]. This reaction is known as the Norrish I type. In this case, the UV radiation brings enough energy to break the single bond

between the two carbons. Hence, two free radicals are created. We call them free radicals because they have one available electron on their external layer, this makes them very reactive. The alkyl free radical is mostly used to take part of the step called initiation.

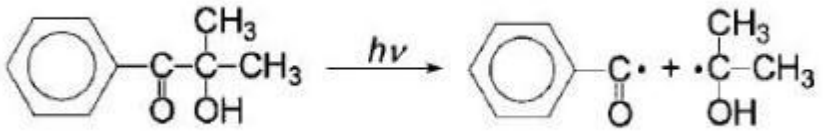

Figure 7: Formation of free radical from the decomposition of a radical photoinitiator molecule [30]

The resin undergoes the reaction of chain propagation until termination. For free radical mechanisms, most of polymer networks are created from unsaturated resins like acrylate or methacrylate resins [18 - 20].

In presence of oxygen, radicals rather get involved into an oxidation reaction than the curing reaction once they have been initiated [23]. Then the rate of curing is reduced and a longer time of exposure is required. Properties are also lowered on surface. Making a layer of nitrogen gas is the most efficient technique found to solve this problem.

Cationic reaction:

Epoxy resins are common thermosets made from cationic reaction. They have many applications like coating, laminates, semiconductor devices, matrix material in composites… The cationic mechanism consists of creating the network by ring opening of an epoxide cycle [24 - 27] (Figure 8).

For a cationic reaction, the initiation step is carried out by creating a carbocation from which the polymer chain is made. In our case, we used stable cations to make the initiation. When they are exposed to UV light, Lewis acids (here SbF_6^-), which are part of the initiator molecule, turn into carbocations (H^+X^- on Figure 8).

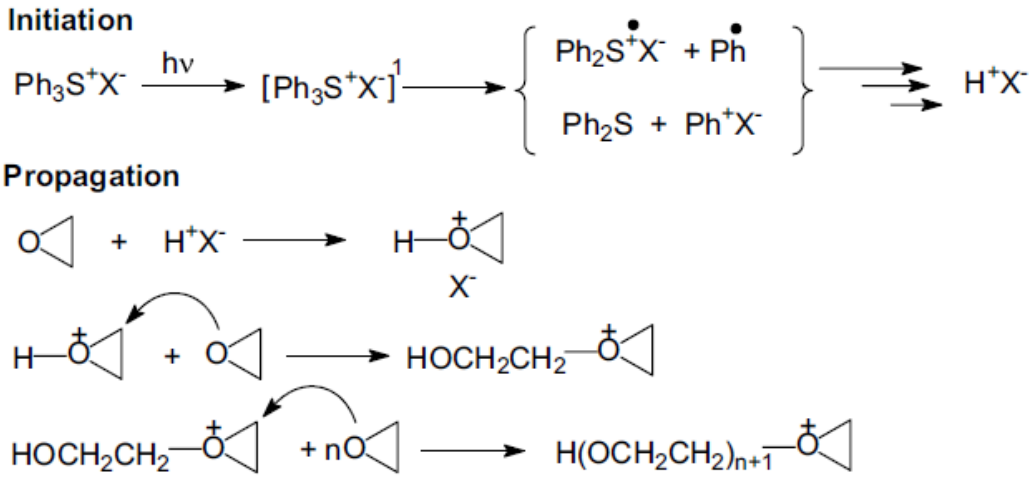

Figure 8: Initiation and propagation mechanisms of the cationic network [26]

Playing with two different mechanisms must prevent from any interaction between systems. We will investigate the miscibility of these two crosslinkers, the kinetic of each reaction individually and as a function of the composition. The thermal properties of our materials will be checked using Thermogravimetric Analysis (TGA) and Differential Scanning Calorimetry (DSC). Infrared Spectroscopy (IR) and DSC will provide information about the conversion ratio obtained after curing. Morphologic analysis will be performed by Atomic Force Microscopy (AFM).

Thus the report of this study will be divided as following:

In a first part we will present the experimental part of our work. The chemicals and their mechanisms will be presented. The devices used for the UV-photo-curing and the measurement technics will be introduced as well. And a preliminary study will be presented with a system including crosslinker and monomer.

In a second part, we will present the results of analyses of UV-photo-cured blend resins. Since this Master thesis implies two degrees from two different universities, the University of Rouen (France) and the University of Lincoln-Nebraska (United States of America), we will show results obtained from both places. Then we will discuss on these previous results.

And a third part will allow us to make a conclusion on our work concerning the miscibility of two thermosetting resins. We will be able to suggest hypotheses on the future work of this 3-year project that just started.

Chapter 2

Experimental

2.1. Materials

Photo-curing was chosen since it allows a dimensional control of photo-initiation compared to thermal curing which uniformly converts big volumes of resin. Moreover as explained previously, UV-photo-curing is easy to manage and very fast. In order to facilitate the initiation of the reaction, we worked with a polychromatic UV lamp emitting in a wide range of wavelengths. Our concern is to make sure of simultaneous curing and of the miscibility of the two resins. We wanted to check out this miscibility over a range of relative proportions with different temperatures.

Radical reaction:

It needs a crosslinker to form the radical network and a free radical initiator to start the reaction; both were purchased from Sigma-Aldrich®.

The photo-initiator is shown on the Figure 9. It is a 2-Hydroxy-2-methylpropiophenone (commercial name: Darocure 1173®).

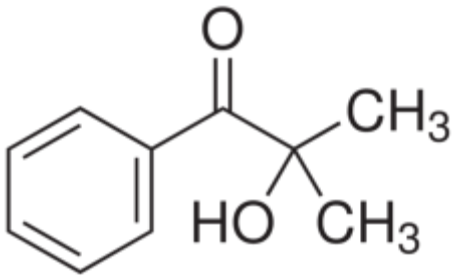

Figure 9: Representation of 2-Hydroxy-2-methylpropiophenone (Sigma-Aldrich®)

Bisphenol A propoxylate diacrylate was used as the crosslinker. Its chemical representation is shown on the Figure 10 and it has a molecular weight of 452.55 $g.mol^{-1}$. When free radicals are formed, they break the double bond on the edge of the acrylate function and alloy the formation of a network as shown on the Figure 11.

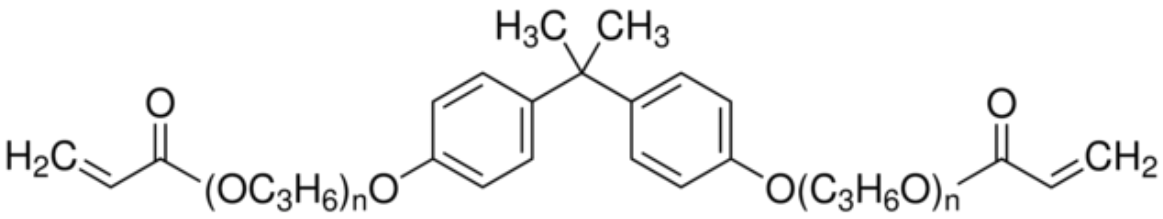

Figure 10: Representation of Bisphenol A propoxylate diacrylate (Sigma-Aldrich®)

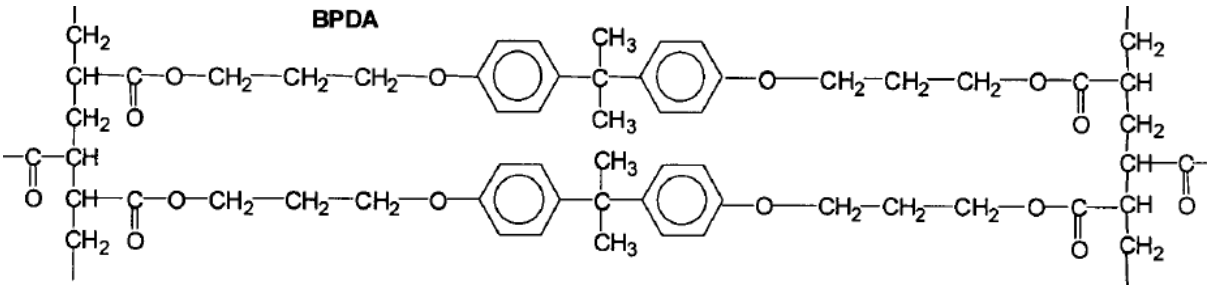

Figure 11: Representation of the formation of the radical network [28]

Cationic reaction:

We used Triarylsulfonium hexafluoroantimonate salts as a photo-initiator (Figure 12). It has been formulated to absorb and initiate in a wide domain of wavelength. Its molecular weight is 1632 $g.mol^{-1}$.

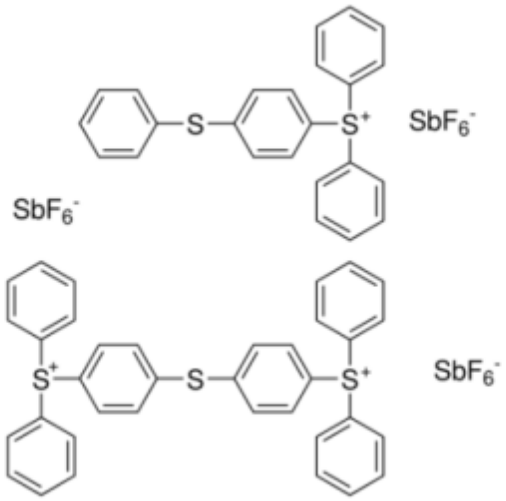

Figure 12: Representation of Triarylsulfonium hexafluoroantimonate salts (Sigma-Aldrich®)

As shown on the Figure 13, the crosslinker we used is a 3,4-epoxycyclohexylmethyl 3,4-epoxycyclohexane carboxylate with a molecular weight of 252.31 $g.mol^{-1}$. The presence of two cycloaliphatic groups in the molecule makes it very reactive. When a carbocation is generated at the initiation, it reacts with the oxirane group and the epoxy function is opened. The crosslinker molecules can then connect to each other.

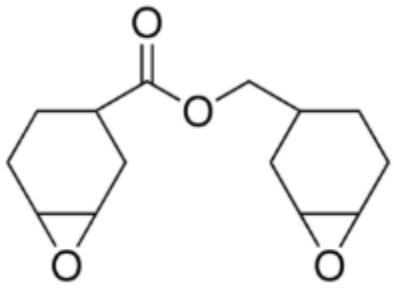

Figure 13: Representation of 3,4-epoxycyclohexylmethyl 3,4-epoxycyclohexane carboxylate (Sigma-Aldrich®)

Light source:

To carry out the photo-curing, we used a Dymax® 5000 flood metal halide lamp emitting ultraviolet radiations (UV-A). The spectrum of the lamp is shown on the Figure 14. Metal halide lamps are similar to mercury vapor lamps but contain additional metal compounds in the arc tube. The power of the lamp is 400 Watts and the intensity of the lamp is equal to 100 mW/cm^2 for a distance lamp/sample equal to 5 inches (12.7 cm).

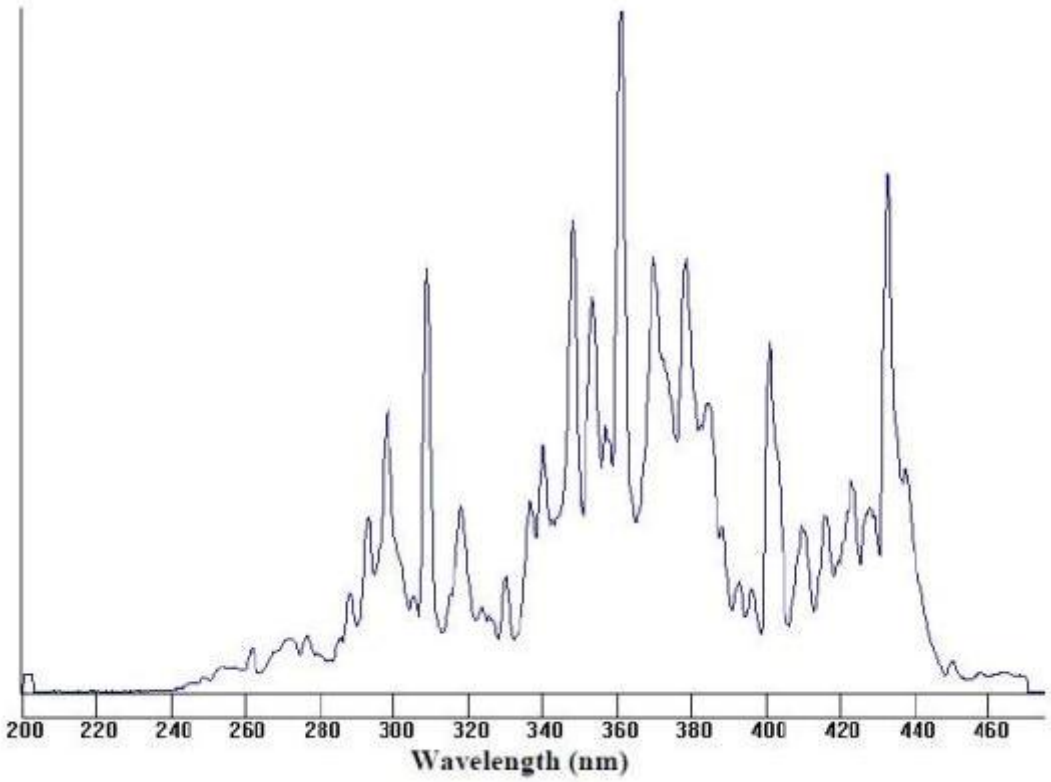

Figure 14: UV spectrum of the metal halide lamp used for experiments

Each photo-initiator has been chosen to be excited at wavelengths compatible with the emission spectra of this polychromatic lamp. They are sensitive to UV radiations between 254 nm and 365 nm.

2.2. Sample preparation

To study the influence of relative proportion of the components, we prepared sets of samples with different weight percentages from 100% cationic to 100% radical. The shape of the analyzed samples below was disc. The dimensions were 6 cm diameter with a thickness of 1 mm. The mixture was made in an aluminum pan and stirred until having a homogeneous solution.

In regard to repeatability, a similar process was used for all the samples as follows. First, the UV light source was switched on at least 10 minutes before exposure to make sure it is stabilized. Mixtures were prepared into the aluminum pans using a scale in respect to weight ratios between radical and cationic crosslinker with an accuracy of 0.01 g. They were manually stirred using a glass stick to homogenize them. If air bubbles got trapped in the resin during the stirring step, the mixture was put under vacuum to get rid of them. Meanwhile, the temperature was increased up to 50°C for a few seconds only to reduce the viscosity and improve the molecular mobility. We also assume that increasing the temperature during the stirring gets rid of humidity since cationic reactions are sensitive to humidity [29]. The homogeneous mixture was placed in the closed UV chamber under nitrogen atmosphere (Figure 15) for 5 minutes before exposure because radical reaction is sensitive to oxygen [30]. We assume that nitrogen kept oxygen away. Thus the mixture was exposed under UV light for 3 minutes under nitrogen at room temperature. Aluminum screens, lab coat, gloves and UV protective glasses were used to ensure the security and the good health of the technicians.

Other sets of samples followed the same process but were exposed at higher temperature (80°C) to investigate the influence of temperature on the curing process. In order to reach a homogeneous temperature in the bulk, a heater was placed in the UV chamber, as seen on the Figure 15. When the temperature of the device was stabilized to obtain a mixture measured at 80°C using a thermocouple, the pan was placed on it just before closing the chamber and blowing nitrogen for 5 minutes.

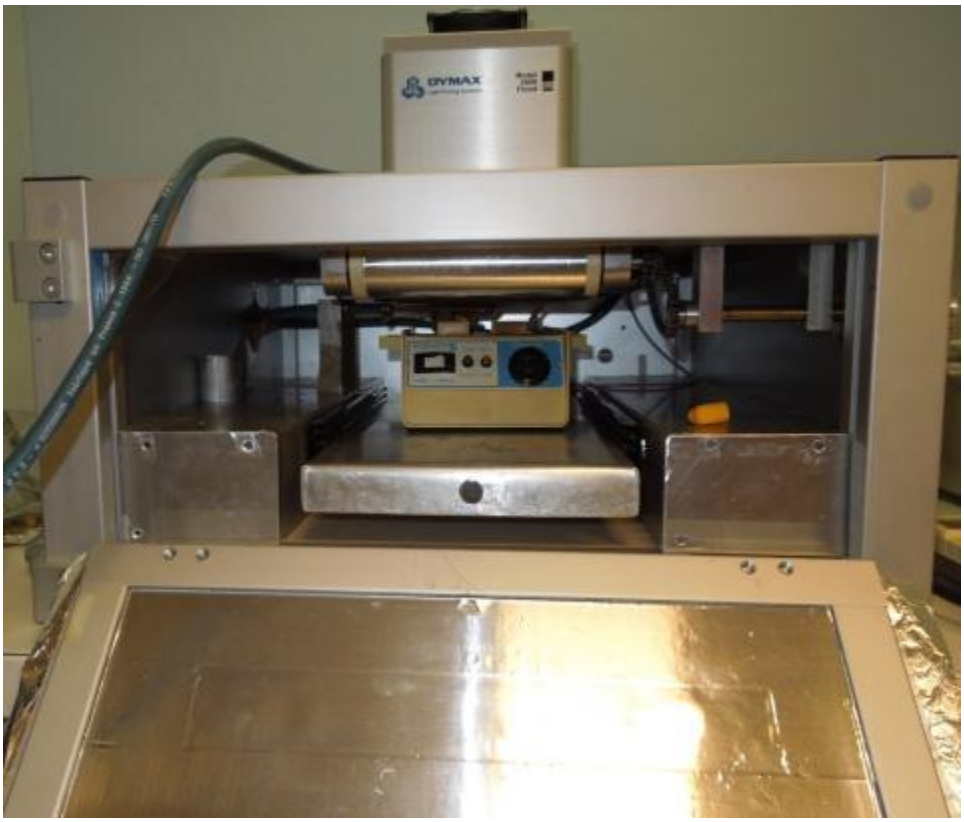

Figure 15: Picture of the UV chamber used for experiments

2.3. Methods

Thermogravimetric Analysis (TGA):

Thermogravimetric Analysis (TGA) is used to study thermal stability of materials. It measures mass variations of a sample which is submitted to a linear variation of temperature as a function of time under controlled atmosphere. The sample mass is around 10 mg. The sensibility of the thermobalance is in the µg range. The curve obtained shows the percentage of mass loss in function of the increasing temperature. The kinetics of this mass loss can be given by the derivative of the previous curve. This technic allows us to know the degradation steps of materials and their associated temperatures. It allows also identifying possible modifications of thermal stability and degradation kinetics in blends compared to pure materials. All the analyses were performed with a device NETZCH® TG209 (Figure 16), in the dynamic mode from 30°C to 700°C at 10°C.min^{-1} under nitrogen at atmospheric pressure.

As an example, the Figure 17 shows typical curves of analyzed samples. The sample mass loss is drawn in blue. This curve is used to determine the onset degradation temperature (T_{onset}), which corresponds to the start of the main degradation of the material. We also find the residual mass, which is the sample mass after the full degradation process. In red is drawn the derivative signal of the sample mass, which corresponds to the kinetics of the degradation. It gives us the moment when the maximum amount of material was degrading. This is the peak temperature (T_{peak}).

Figure 16: picture of the TGA TG209 from NETZCH

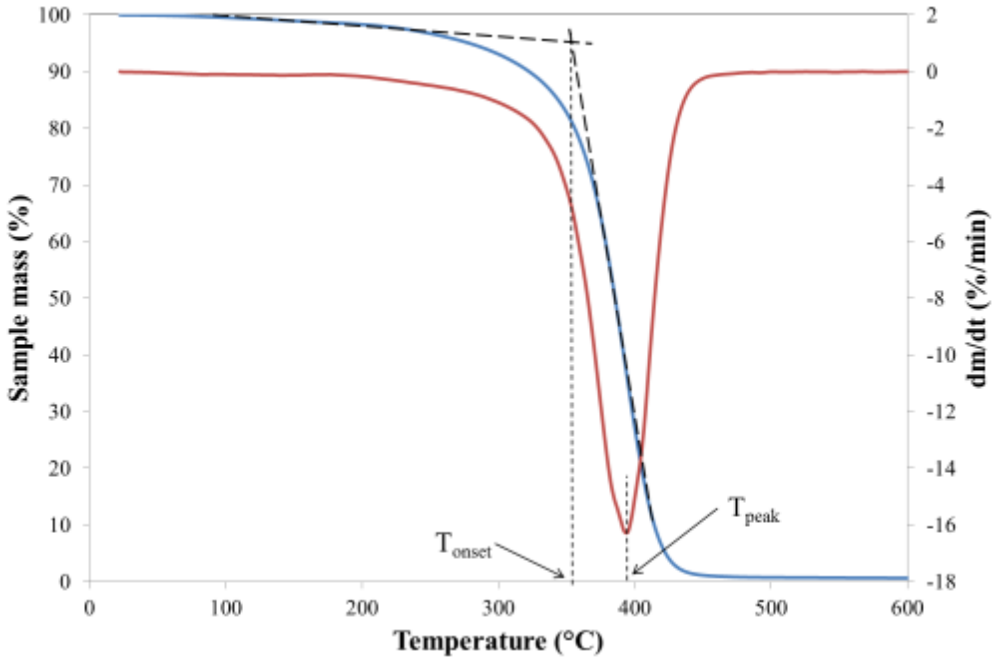

Figure 17: Thermogravimetric curves of sample mass (blue (●)) and derivative sample mass (red (●)) of a cationic resin

Differential Scanning Calorimetry (DSC):

Differential scanning Calorimetry (DSC) is a technique allowing the qualitative and quantitative analysis of thermal phenomena related to phase transitions or structural changes in a material. We first used a heat flow device TA® Q100 (Figure 18). The sample and a reference pan are placed in a single furnace and are submitted to a same temperature program. A thermocouple made of an alloy of chrome and nickel measures the heat flow difference between these two pans. This technique allows low heating and cooling rates. Its high resolution measurement is adapted to lowly crosslinked systems but its sensibility is too weak to analyze systems with a very low ΔCp.

So we used a power compensation device PERKIN-ELMER® 8500 (Figure 19). This double furnace design (one containing the sample and the other containing the reference) is lower in volume so it is possible to apply high heating and cooling rate while keeping fast thermal response. The thermal sensors are platinum resistance thermometers. Measurement consists to register the power variations resulting from heat flow exchanges between the reference and the outside on one hand and between the sample and the outside on the other hand. Calibration includes 3 steps:

- Baseline correction.
- Calibration in temperature using standards of indium (Tf = 156.6 °C) and benzophenone (Tf = 48°C) as reference.
- Calibration in energy using the melting enthalpy of indium (ΔHf = 28.66 J/g) as reference.

Figure 18: Picture of the DSC Q100 from TA (source: Premier Laboratory Services Inc.)

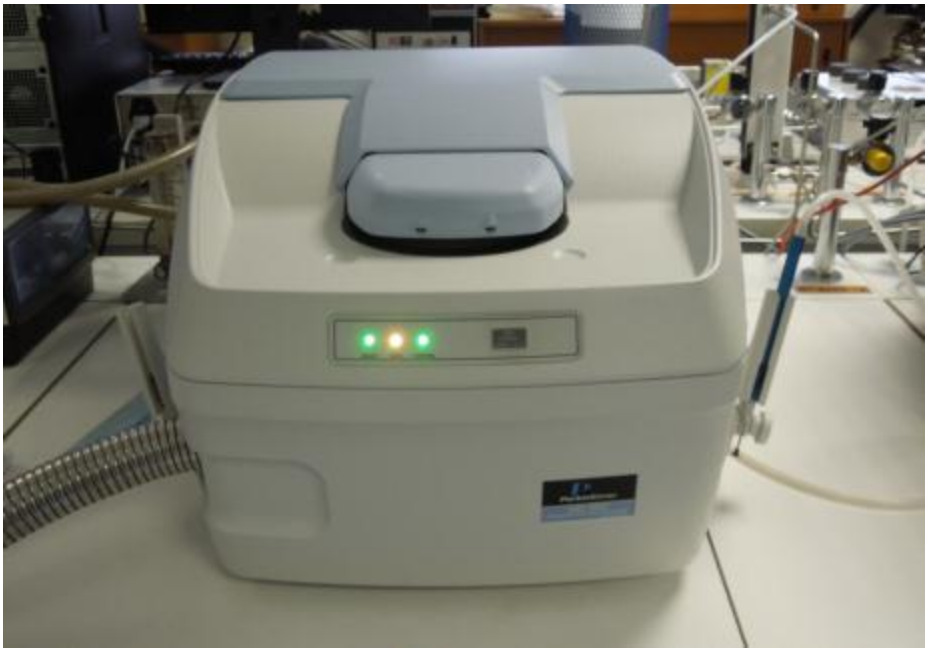

Figure 19: Picture of the DSC 8500 from PERKIN ELMER

The glass transition of thermoset resins is often hard to detect as the corresponding heat capacity step value is low. Keeping in mind that our priority is to assure the detection of all thermal events, we have chosen to increase the sensibility of the analysis by working with high heating rate (50K/min) and with a relatively high sample mass (ranging from 10 to 20 mg). All experiments were carried under nitrogen atmosphere (30 mL/min).

Indeed, DSC analysis was performed on a radical polymer sample containing 71.25 wt.% of radical crosslinker, 28.25 wt.% of radical monomer and 0.5 wt.% of photo-initiator using a DSC analyzer Q100 from TA with a heating rate of 10 K/min. Measurements were realized on a sample with a mass of 6 mg and under nitrogen atmosphere (20 mL/min). This device has a great resolution but you can see on the Figure 20 that the sensibility is very bad. The Tg was detected with a ΔCp of 0.08 mW/g. Analyses with a high speed DSC will increase this ΔCp.

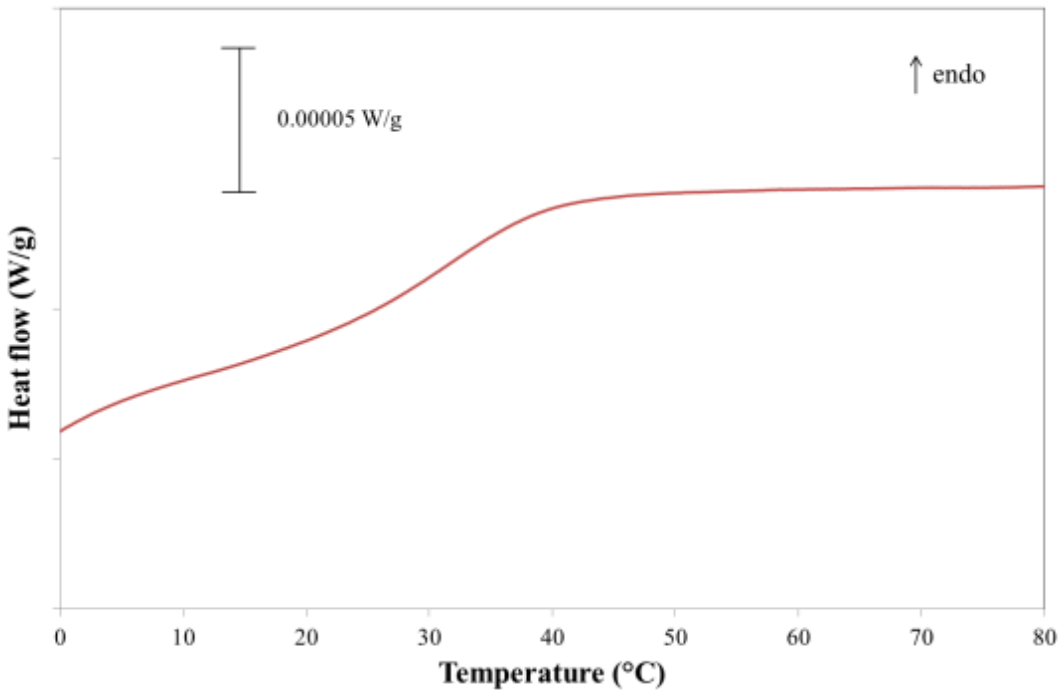

Figure 20: DSC of a radical polymer by a DSC TA Q100

DSC can also help picturing the conversion ratio. In Figure 21 are presented the first (above) and the second (below) heating run (at 20 K/min) performed on a cured epoxy resin [31]. A significant 30°C shift of the glass transition temperature is observed from the first analysis to the second one. This is explained by the presence of a wide exothermic peak following the glass transition on the above curve. This peak is characteristic of thermal post-curing following the network relaxation process. The consequence of this post-curing is to harden the material and to increase the glass transition temperature. This behavior is specific to the cationic cured systems.

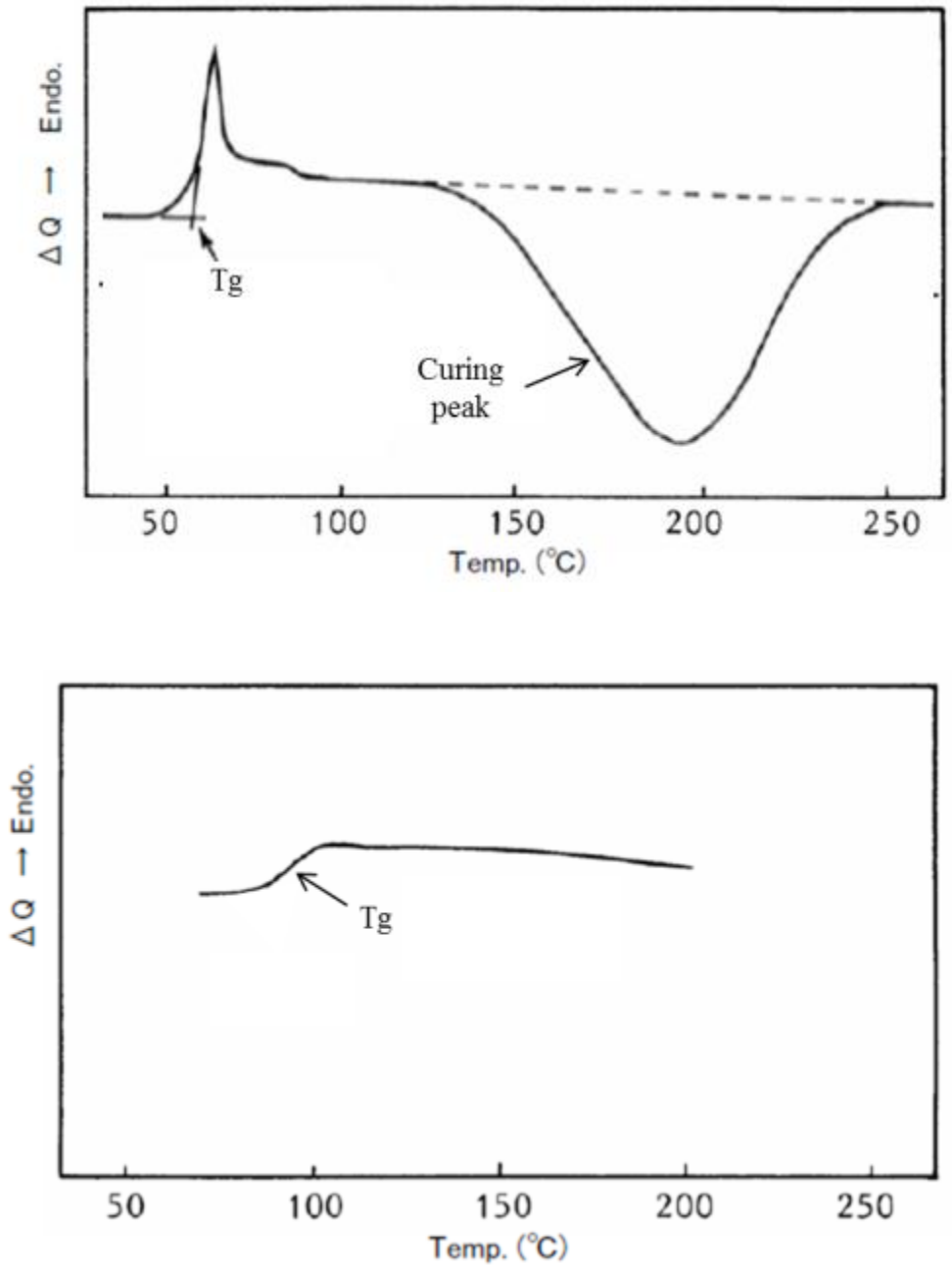

Figure 21: DSC curves of a cured epoxy resin, first run above and second run below

Fourier Transformed InfraRed Spectroscopy (FT-IR):

Spectroscopy analyses were carried out with a Varian® 4100 FT-IR (Figure 22) apparatus from Excalibur® series. The measurement was done in absorption mode including 16 scans. The resolution was about 0.25 cm^{-1}.

A FTIR spectrometer generates spectral data from absorption of liquid or solid specimens. This machine is producing light over a broad range of infrared wavelengths. The wavelength is then selected by an interferometer. An infrared detector measures the intensity of the light which was not absorbed by the sample. Molecules have specific rotation and vibration frequencies in infrared domain related to their dipole moment. Qualitative and quantitative chemical analysis can be realized by measuring vibration modes and their intensities.

The Attenuated Total Reflectance (ATR) mode was used in all the measurements. It consists of submitting many reflections of an IR beam to the interface between the sample and a crystal. This mode allows studying samples in their natural state without any preparation.

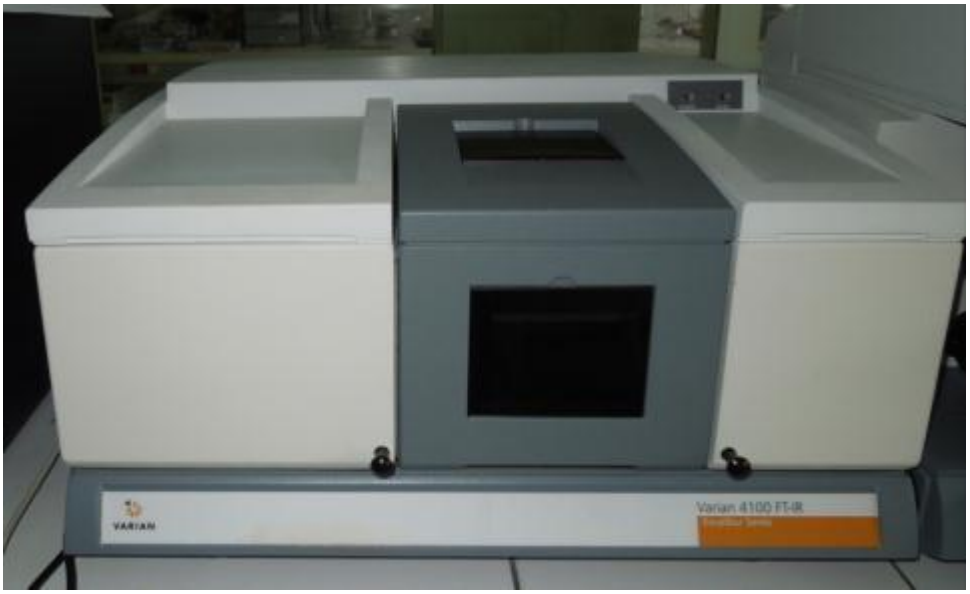

Figure 22: Picture of FTIR spectrometer from VARIAN

In our case, infrared spectrometry will be used to determine a conversion rate. This conversion rate gives information about the level of curing of the polymer. During the reaction, only a few functions of the molecule are involved. They disappear to build new functions. A conversion rate can be determined by tracking the peaks related to these disappearing functions before and after the reaction. To insure a good repeatability, the intensity of these peaks is normalized to an invariant peak, which corresponds to a function that is not concerned during the curing reaction.

As an example, the Figure 23 shows the spectra of the cationic resin before and after curing. Both were normalized to an invariant peak appearing around 1700 cm^{-1}. More details about the specific functions will be presented later. A peak located around 790 cm^{-1} was tracked. It corresponds to the main function involved, which is supposed to disappear. After the photo-curing, we observe using the red spectrum that this function is

not fully disappeared. The reaction was not total. Therefore a conversion rate can be calculated.

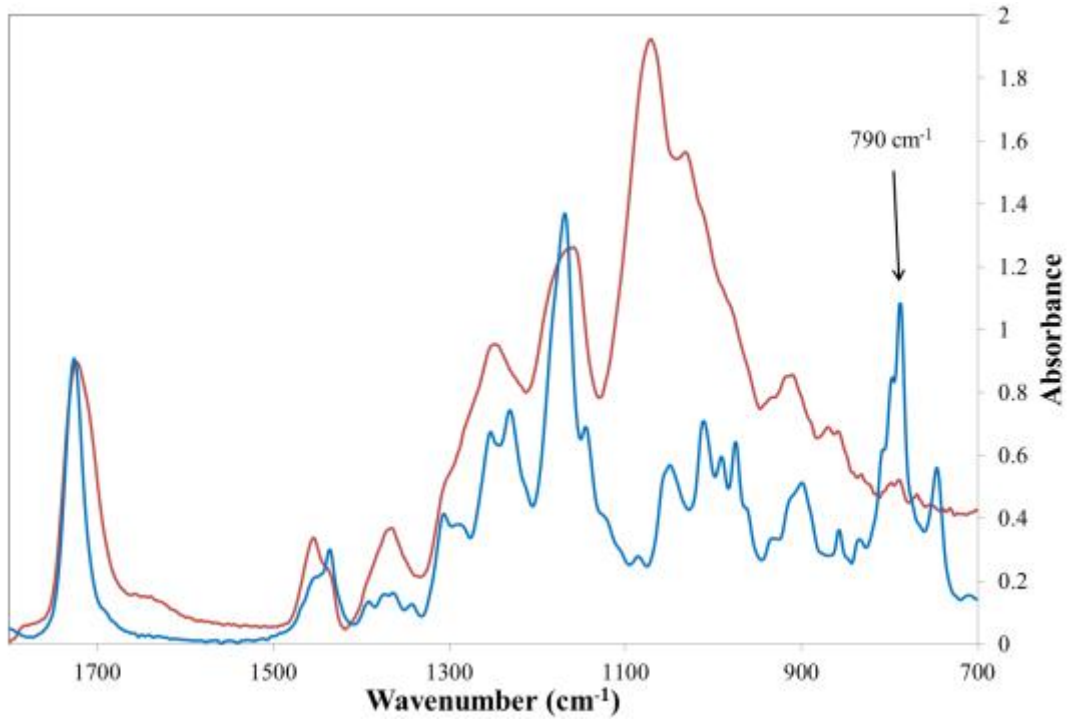

Figure 23: ATR FTIR spectra of cationic resin before (in blue: ●) and after (in red: ●) photo-curing

Atomic Force Microscopy (AFM):

AFM measurements were performed by Wenlong Li, who is part of the project, using a Nanoscope IIIa Dimension 3100 SPM by Digital Instruments (Figure 24). This technic is appreciated to take a look at the morphologic aspect of materials and check its homogeneity at the microscopic scale. The scanning probe is made of etched silicon and has a resolution on the order of 0.5 nm. It is made of a sharp tip cantilever placed into proximity of the analyzed sample. Forces generated between the particles of the tip and the ones of the sample lead to a deflection of the cantilever, which are following the elastic Hooke's law ($\sigma = E\varepsilon$, with σ the stress, E the Young modulus and ε the strain). This deflection is recorded and transformed using a laser reflecting on top of the probe to a photo-diode array. This high resolution machine allows contact and non-contact modes of measurement.

We used a non-contact mode called the tapping mode. It consists of making the probe oscillate up and down near the sample surface using a piezoelectric element. When the tip goes close to the surface of the sample, the amplitude of oscillations is decreasing. The piezoelectric part is then used to control the distance between the tip and the sample. Hence, the AFM tapping image is produced by mapping the intermittent contact of the tip on the sample surface.

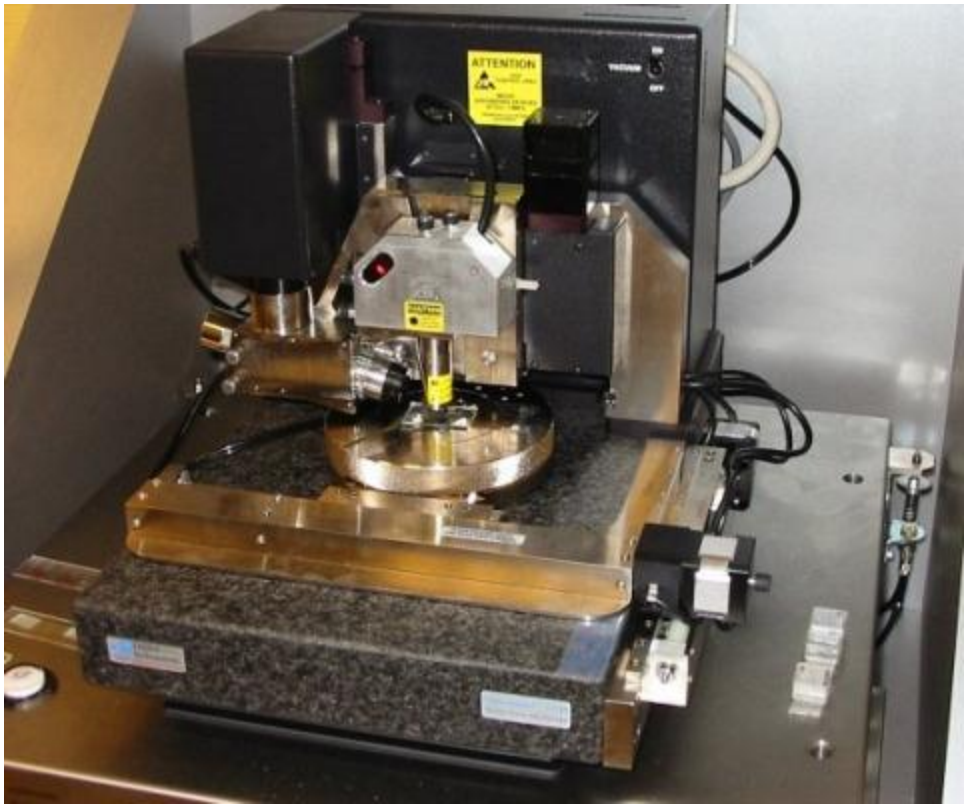

Figure 24: Dimension 3100 SPM AFM device from Digital Instruments (Source: Centre Commun de Microscopie de Lille)

Chapter 3

Results

The importance of nitrogen gas flow to lead the photo-curing was noticed. A set of samples was manufactured with a reduced nitrogen flow. As a result, the final materials were sticky, which means that no reaction occurred on the surface.

All the samples which are analyzed below are presented in the Table 1. The received ones are checked and a column was made to justify the rejection of the failed ones. Let's remain that Bisphenol A propoxylate diacrylate and 2-hydroxy-2-methylpropiophenone 97% were used respectively as radical crosslinker and photo-initiator. 3,4-epoxycyclohexylmethyl 3,4-epoxycyclohexane carboxylate and Triarylsulfonium hexafluoroantimonate salts mixed (50 wt.% with propylene carbonate) were used respectively as cationic crosslinker and photo-initiator.

Radical/Cationic crosslinkers ratio (wt. %)	Radical (weight in g)		Cationic (weight in g)		Atmosphere & temperature	Decision
	Crosslinker	Photo-initiator	Crosslinker	Photo-initiator		
25/75	0.75	0.015	2.25	0.015	N_2+O_2 - 20°C	Rejected
25/75	0.75	0.015	2.25	0.015	N_2+O_2 - 20°C	Rejected
50/50	1.5	0.015	1.5	0.015	N_2+O_2 - 20°C	Rejected
50/50	1.5	0.015	1.5	0.015	N_2+O_2 - 20°C	Rejected
75/25	2.25	0.015	0.75	0.015	N_2+O_2 - 20°C	Rejected
75/25	2.25	0.015	0.75	0.015	N_2+O_2 - 20°C	Rejected
0/100	0	0.018	3	0.018	N_2 - 20°C	Accepted
15/85	0.45	0.018	2.55	0.017	N_2 - 20°C	Accepted
25/75	0.75	0.015	2.25	0.018	N_2 - 20°C	Accepted
32/68	1.02	0.017	1.98	0.019	N_2 - 20°C	Accepted
40/60	1.2	0.016	1.8	0.016	N_2 - 20°C	Accepted
45/55	1.35	0.019	1.65	0.019	N_2 - 20°C	Accepted
50/50	1.5	0.014	1.5	0.013	N_2 - 20°C	Accepted
60/40	1.8	0.012	1.2	0.013	N_2 - 20°C	Accepted
75/25	2.25	0.015	0.75	0.019	N_2 - 20°C	Accepted
100/0	3	0.015	0	0	N_2 - 20°C	Accepted
0/100	0	0	3	0.06	N_2 - 80°C	Accepted
25/75	0.75	0.0015	2.25	0.045	N_2 - 80°C	Accepted
40/60	1.2	0.0024	1.8	0.036	N_2 - 80°C	Accepted
50/50	1.5	0.003	1.5	0.03	N_2 - 80°C	Accepted
60/40	1.8	0.0036	1.2	0.024	N_2 - 80°C	Accepted
75/25	2.25	0.0045	0.75	0.015	N_2 - 80°C	Accepted
100/0	3	0.006	0	0	N_2 - 80°C	Accepted

Table 1: Table of the samples prepared during the study

3.2.1 Atomic Force Microscopy (AFM):

The Figure 25 shows a tapping AFM image of a sample containing 50 % of radical resin and 50 % of cationic one. It was irradiated by UV for 30 seconds. We can see some dispersed white spots which look similar and could be assigned to the radical network. The matrix is composed of regularly scattered black and white stripes. We know that cationic resins usually need a thermal post-cure to be fully cured. So these stripes might correspond to cured and uncured resin. Analysis of thermal properties by DSC can help to verify this assumption.

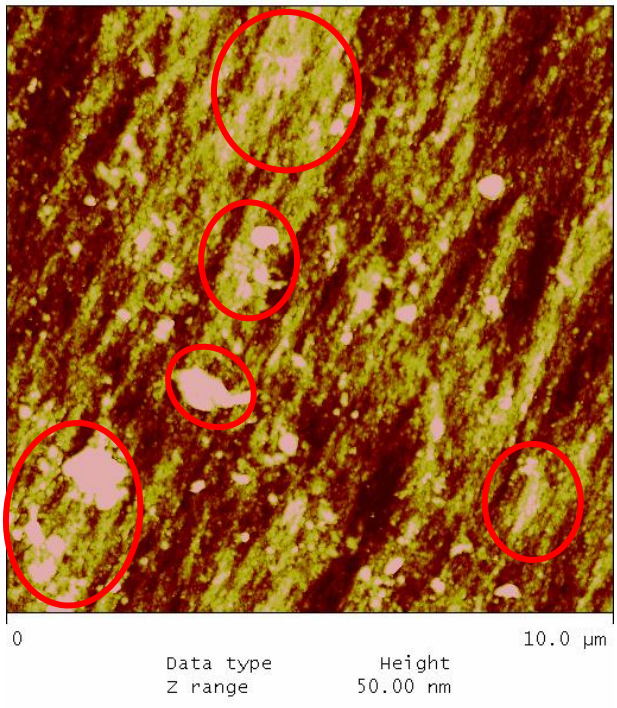

Figure 25: Tapping AFM image of the sample containing 50 % radical

The Figure 26 shows a tapping AFM image of a sample containing 25 % of radical and 75 % of cationic compound. We notice the same kind of texture as the 50 % image. But the white part seems more important and uniform. We can even more think that it is related to the cationic part. But the technic is still unable to help us to assign the white and the black areas. There is less white spots previously assigned to the radical network. But these spots look bigger than before. The high majority of cationic compound might have helped them to assemble.

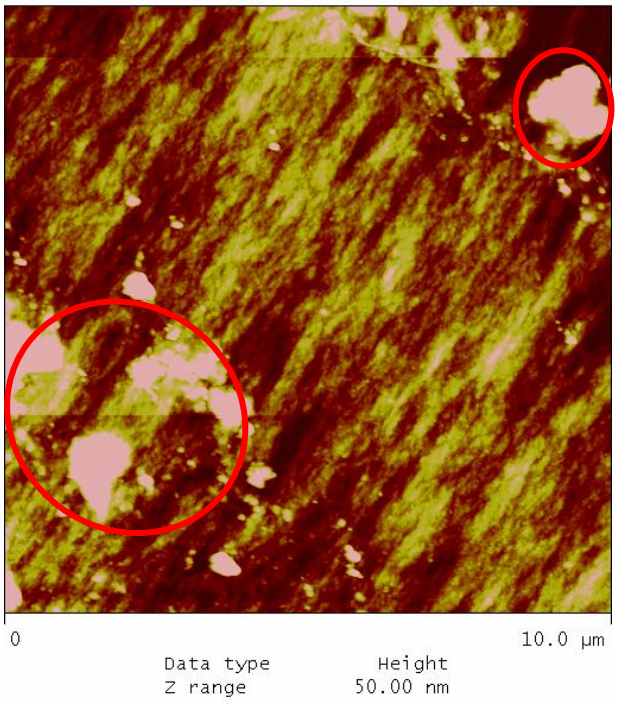

Figure 26: Tapping AFM image of the sample containing 25 % radical

3.2.2 Fourier Transform Infrared spectroscopy (FTIR)

FTIR spectroscopy analyses were performed on the pure resins then blends containing 25 wt%, 40 wt%, 50 wt%, 60 wt% and 75 wt% radical crosslinker. Two sets of samples were respectively photo-cured at 20°C and at 80°C. The non-cured pure resins were analyzed as well.

In Figure 28 are presented the three spectra for the pure cationic resin. It can be used to see the influence of the curing temperature on the chemical structure. Indeed, previous investigations studied the system 3,4-epoxycyclohexylmethyl-3,4-epoxycyclohexane carboxylate by FTIR spectroscopy [24 - 26]. It was proved that the peak at 1730 cm^{-1} corresponds to an invariant carbonyl bond (Figure 27). The band at 1070 cm^{-1} corresponds to a stretching vibration of ether. It increases during the reaction while around 790 cm^{-1}, the absorption band of epoxy ring is decreasing when the curing occurs. Actually, the epoxy ring (or oxirane) disappears to make an ether group during the curing. This ether bond is used to connect the crosslinker molecules together. The conversion rate is used to be tracked with the epoxy decreasing band. The signals were normalized to the carbonyl absorption band.

On the spectra, we can see that a fewer amount of epoxy groups reacted during the curing at 20°C than during the one at 80°C. We can estimate a conversion rate by comparing the intensity of both epoxy bands uncured and cured since spectra are normalized to the intensity of the invariant band from carbonyl. We used the next formula: $conversion\ \% = \left[1 - \frac{Hight_{cured\ epoxy}}{Hight_{uncured\ epoxy}}\right] * 100$. Using this approximation, it turns out that the cationic resin was 55 % and 92 % cured at 20°C and 80°C respectively.

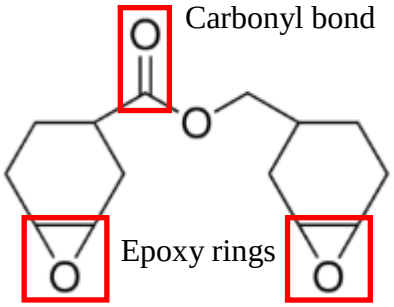

Figure 27: Chemical bonds used to estimate the conversion rate of curing of 3,4-epoxycyclohexylmethyl-3,4-epoxycyclohexane carboxylate

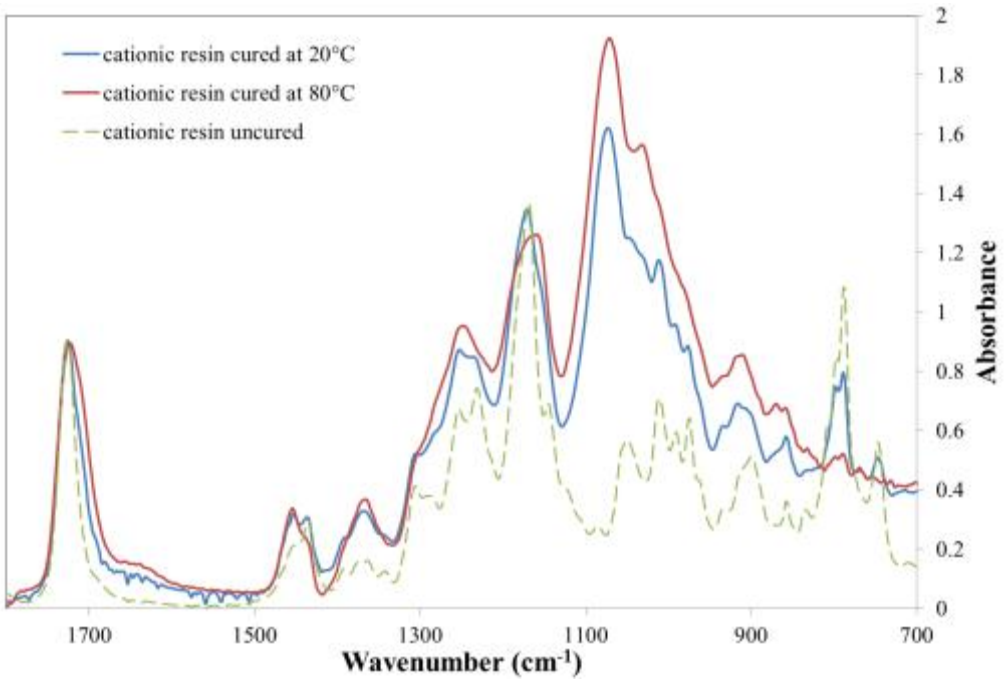

Figure 28: ATR FTIR spectra of 100% cationic resin. Blue (●): cationic resin cured at 20°C; Red (●): cationic resin cured at 80°C; Dashed green (●): uncured cationic resin.

The conversion rate of cationic resin is not possible by FTIR in the blends since the spectrum of the radical part is altering the signal of the cationic resin. Indeed, as we can

see below on the Figure 29, the radical resin presents a peak of high intensity at 800 cm^{-1}. This peak overlays the epoxy ring peak of the cationic network, which is supposed to decrease as the conversion rate increases. Tracking the conversion rate of the cationic network using FTIR is dropped then.

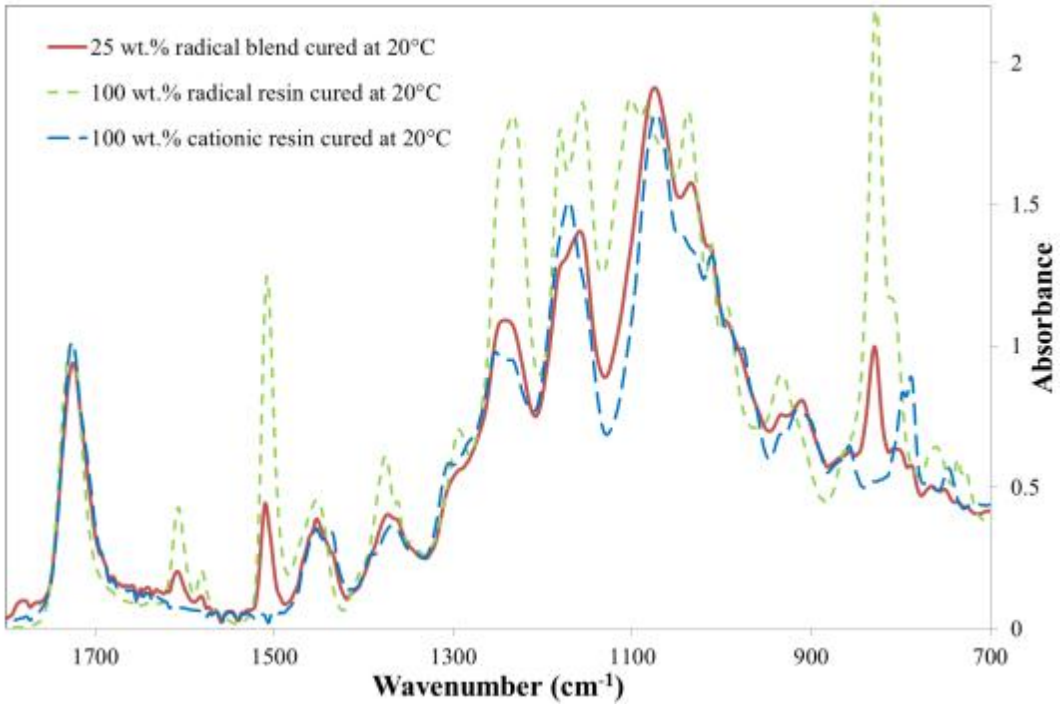

Figure 29: ATR FTIR spectra of: Red (●): 25 wt.% radical blend cured at 20°C; Dashed green (●): uncured cationic resin; Blue (●): cationic resin cured at 20°C.

The degree of conversion of the radical resin wasn't studied because samples were well cured according to their aspect and their process. They were manufactured with a low thickness using a high power UV lamp. Chartoff et al. [32] reported that a majority of the radical resins get cured with a degree of conversion between 60 % and 80 %.

3.2.3 Thermogravimetric Analysis (TGA)

Thermal stability of photo-cured radical resin, cationic resin and blends of different ratios was studied by Thermogravimetric analysis under nitrogen atmosphere. In Figure 30 are shown the curves of 100% cationic, 25% radical, 50% radical, 75% radical, and 100% radical resins. In Figure 33 are shown the derivative of the Thermogravimetric signal, it corresponds to the kinetic of degradation. We put the degradation temperatures and the residuals masses after degradation of all the samples together on the Table 3.

We can tell that all the samples are thermally stable up to 250°C since the mass loss is less than 5%. Thus we assume that we have homogeneous thermosetting systems. Above 500°C, the cationic resin is almost totally degraded (0.5 % residual mass), while the pure radical still has 4 % residual mass.

The blends are describing an intermediate behavior between the two pure resins. Hence their degradation is occurring on a wider temperature range. The second step of degradation is more visible as the ratio of radical content increases. Simultaneously, T_{peak} and T_{onset} are decreasing.

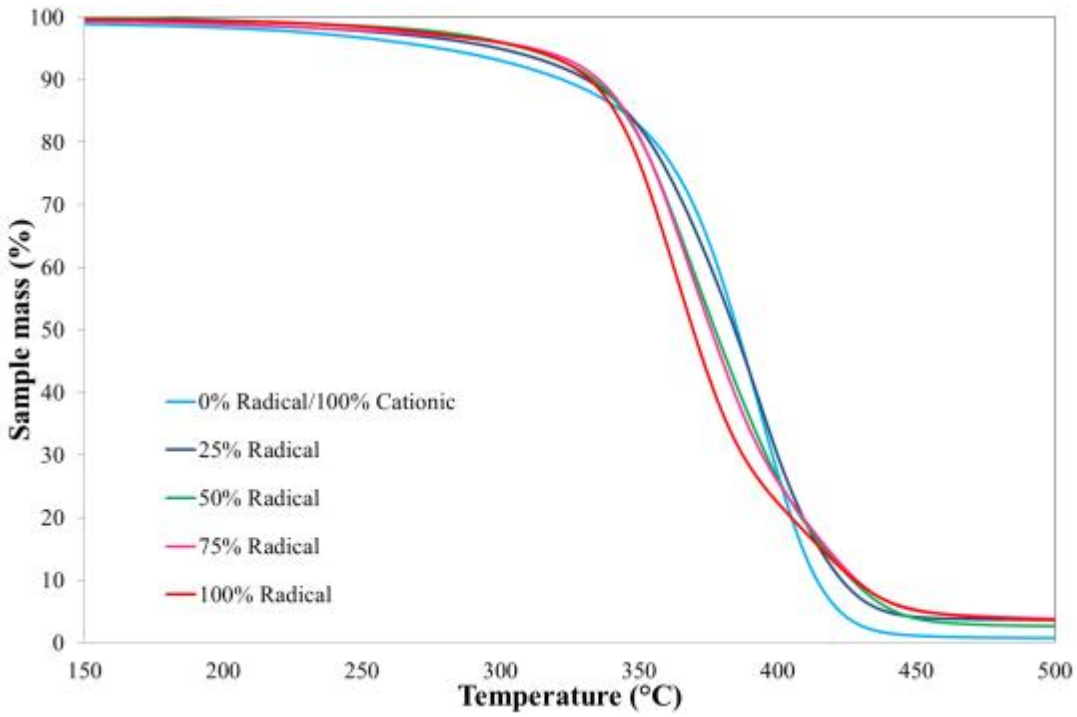

Figure 30: Thermogravimetric curves obtained at 10°C.min^{-1}. Cyan (●): 0% radical; Dark blue (●): 25% radical; Green (●): 50% radical; Pink (●): 75% radical; Red (●): 100% radical.

However, the curves of the blends are not simple mixes of the pure resins ones. There is no linear additive law of the characteristic degradation parameters in function of the contents ratios. For regular blends, thermal behaviors are described by a Flory-Fox relation using the glass transition temperatures of materials [33]. Here we can check this behavior with degradation of materials. Let's study the sample temperature at 50 % mass loss. We can define T_{calc}, which is the temperature of a sample degraded at 50 wt.%, using the equation: $\frac{1}{T_{calc}} = \frac{w_{rad}}{T_{meas,rad}} + \frac{w_{cat}}{T_{meas,cat}}$ with $T_{meas,rad}$ and $T_{meas,cat}$ temperatures of pure radical and pure cationic materials degraded at 50 wt.% respectively. They were measured from Figure 31. w_{rad} and w_{cat} are respectively the weight ratios of radical and cationic components in the blend. Tcalc of the blends are reported into the Table 2.

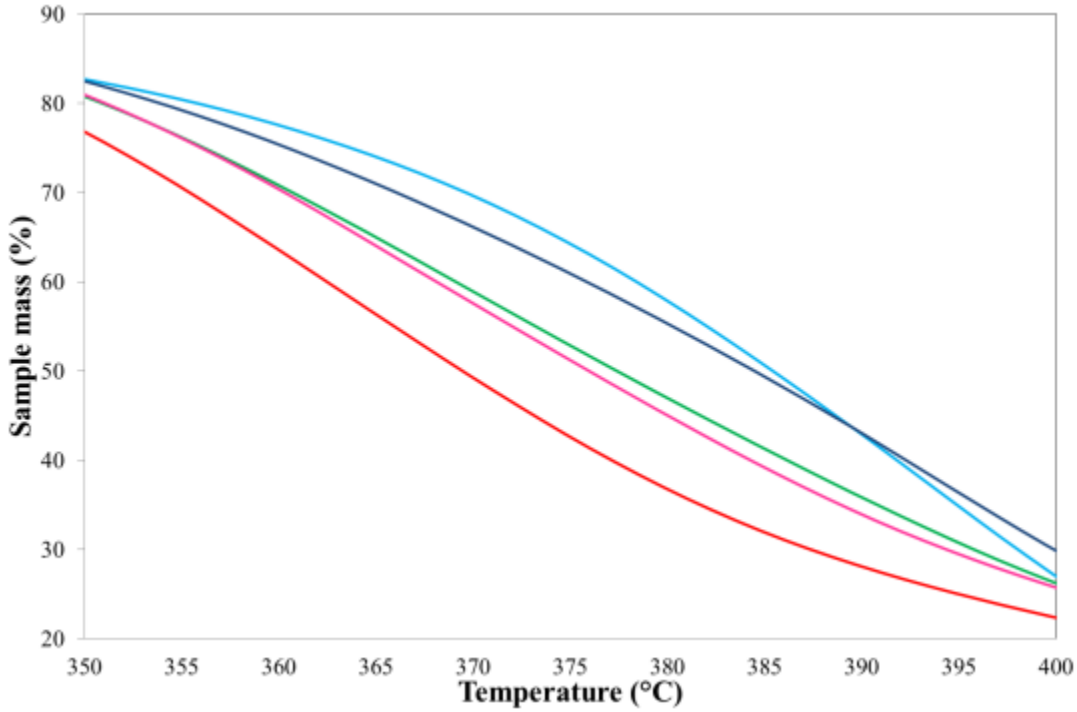

Figure 31: Zoom of Thermogravimetric curves obtained at 10°C.min^{-1}. Cyan (●): 0% radical; Dark blue (●): 25% radical; Green (●): 50% radical; Pink (●): 75% radical; Red (●): 100% radical.

Sample ID	Measured temperature T_{meas} (°C)	Calculated temperature T_{calc} (°C)
0% radical	386	386
25% radical	384	382
50% radical	378	378
75% radical	376	374
100% radical	369	370

Table 2: Degradation temperatures of materials at 50 wt. % loss

The Figure 32 shows the evolution of samples temperatures at 50 wt.% mass loss in function of weight ratio of radical compound. In red, the calculated curve of temperatures is following the linear relation of Flory-Fox.

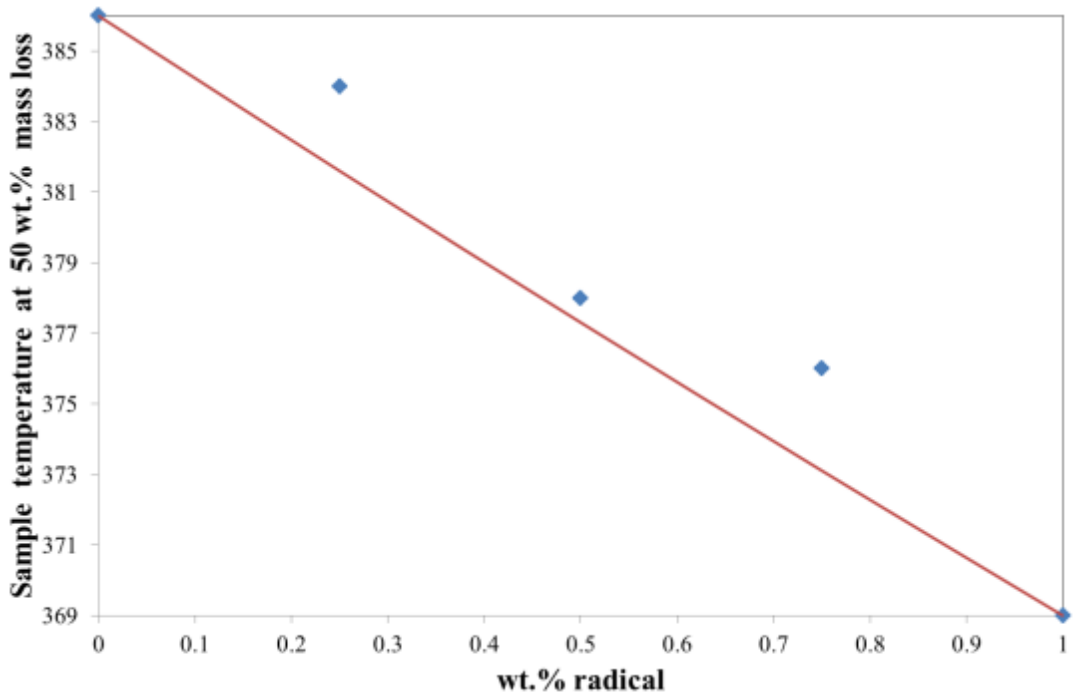

Figure 32: Evolution of calculated (Red (●)) and measured (Blue (●)) sample temperature at 50 wt. % mass loss.

From this, we can suppose that we don't have regular polymer blends and that there exists some interactions between both networks. DSC analyses are able to confirm this hypothesis.

The pure cationic and radical resins are both thermally stable. T_{onset} and T_{peak} of the cationic resin are respectively 20°C and 30°C higher than the pure radical ones (Table 3). In regard of the kinetics of degradation shown on the Figure 33, we can see that the cationic resin has a one-step degradation, whereas the radical compound goes through a two-step degradation.

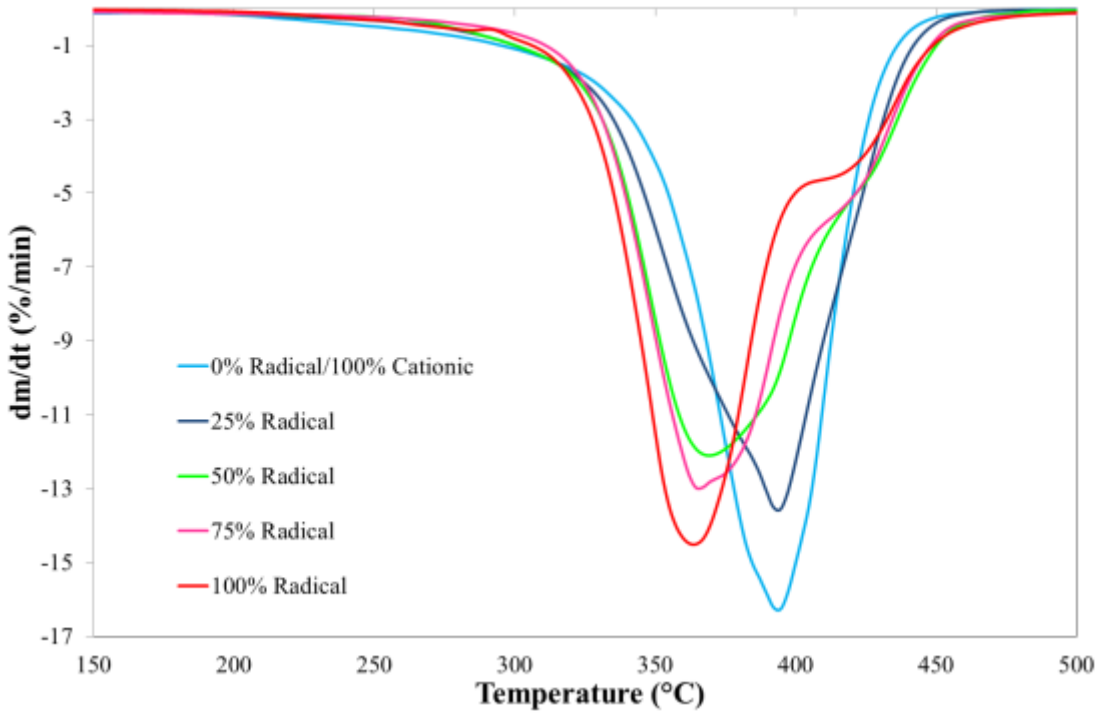

Figure 33: Derivative Thermogravimetric curves obtained at 10°C.min^{-1}. Cyan (●): 0% radical; Dark blue (●): 25% radical; Green (●): 50% radical; Pink (●): 75% radical; Red (●): 100% radical.

	Tonset (°C)	Tpeak (°C)	Residual mass (%)
100% cationic	355	392	0.5
25% radical	345	392	3.6
50% radical	337	367	2.5
75% radical	337	365	3.4
100% radical	335	362	3

Table 3: Thermal stability of polymer blends of different radical/cationic ratio

3.2.4 Differential Scanning Calorimetry (DSC)

In this part, results and DSC curves are presented. Each figure corresponds to a specific ratio between radical and cationic compound. Samples initiated at 20°C (called room temperature) and 80°C are shown on each graph to study the influence of curing temperature on the final properties. For every analyzed sample, two successive DSC analyses were carried out in a row. Those two runs are shown below. These tests can give us thermodynamic information about the material as Tg, ΔTg, ΔCp. Tg is the glass transition temperature, it is characterized by an endothermic step between the glassy state and the rubbery state. The domain of temperature on which the glass transition is spread out is ΔTg. ΔCp is the difference of heat capacity of the material between the glassy and the rubbery state.

The legend is set as follows:

Blue (●): sample initiated at 20°C, run 1

Green (●): sample initiated at 20°C, run 2

Cyan (●): sample initiated at 80°C, run 1

Black (●): sample initiated at 80°C, run 2

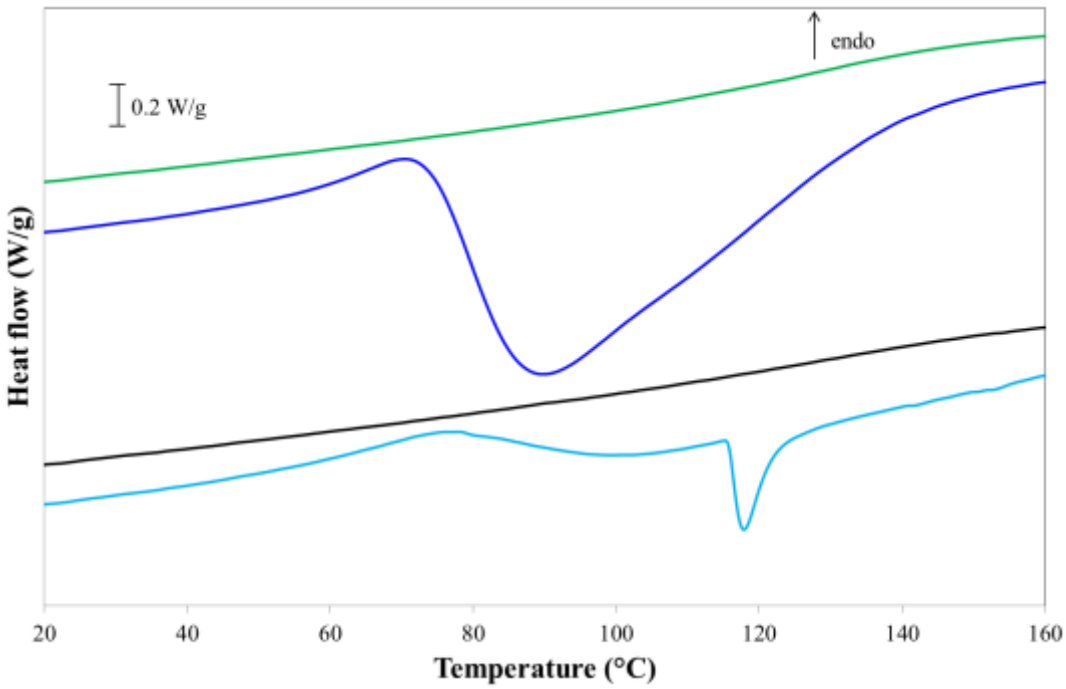

Figure 34: DSC results of a resin with proportions 0:100 wt.% (radical:cationic) initiated at 20°C and 80°C - Blue (●): sample initiated at 20°C, run 1; Green (●): sample initiated at 20°C, run 2; Cyan (●): sample initiated at 80°C, run 1; Black (●): sample initiated at 80°C, run 2

The analysis of the pure cationic resin is shown on the Figure 34. The glass transition of the material is hidden by an exothermic peak on the first run independently on the initiation temperature. This peak appears around 90°C for the sample cured at ambient temperature and is shifted to 120°C for the one cured at 80°C. This peak presence can be justified using the second run of each analysis. Indeed this peak doesn't appear on any second scan. That can be explained as follows: when the sample was submitted to the first heating ramp, some unconverted species finished to react. Indeed, it often happens with photo-curing of thermosets that the conversion rate is very low [24]. Then we can assume that this exothermic peak is a thermal post-curing peak. This is characteristic of photo-curing of cationic resins (Figure 21).

It turns out that the enthalpy of post-curing is higher when the resin was cured at ambient temperature. The enthalpy corresponds to the area of the peak and is measured in J/g. Therefore we can tell that curing the resin at higher temperature pushed the conversion forward.

The second scan shows a Tg 70°C higher than the first scan. That means that the network obtained after thermal post-curing is way more organized and stable. This phenomenon comes with an increase of Tg. In regular polymers, this should come with a weaker ΔCp in the second scan. This parameter is directly related to the molecular mobility in the material, so an increase of the crosslinking must be followed by a decrease of ΔCp. But measurement of ΔCp isn't accurate because of the post-curing peak happening before the end of the Tg. This behavior is interesting and it would be interesting to investigate the conversion rate using a technique like infrared coupled DSC.

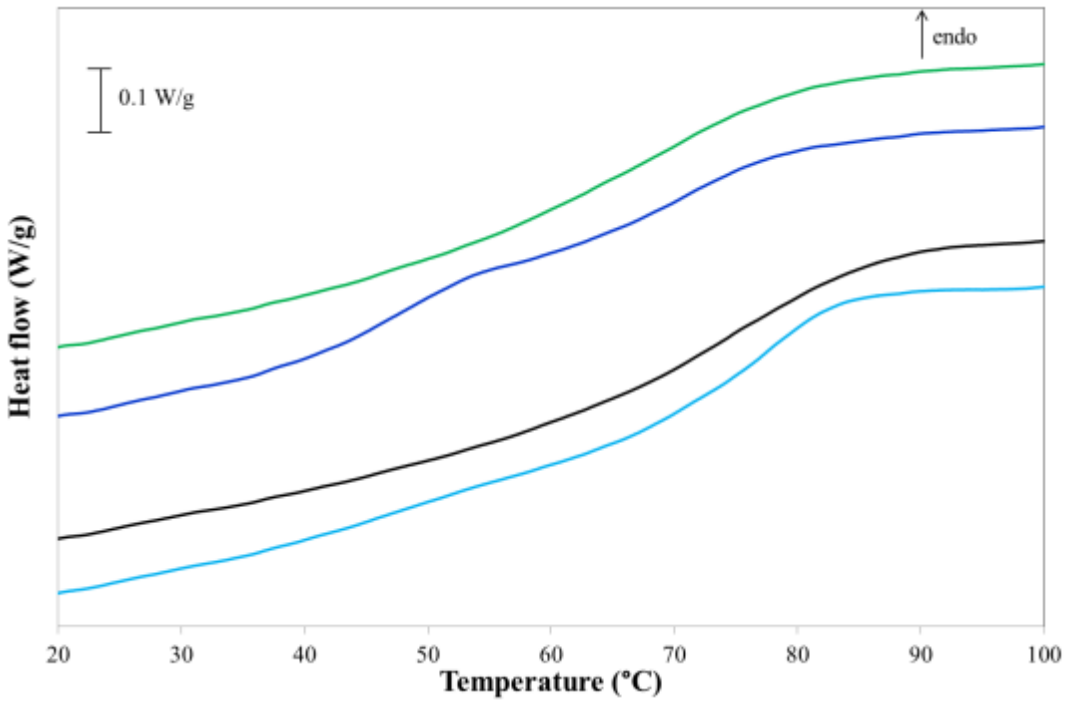

Figure 35: DSC results of a resin with proportions 100:0 wt. % (radical:cationic) initiated at 20°C and 80°C - Blue (●): sample initiated at 20°C, run 1; Green (●): sample initiated at 20°C, run 2; Cyan (●): sample initiated at 80°C, run 1; Black (●): sample initiated at 80°C, run 2

Concerning the pure radical resin shown on Figure 35, two glass transitions are observed during the first and only one during the second scan. Is the molecular structure heterogeneous? The photo-curing might have introduced a distribution of conversion within the core material. After the surface was cured, it might be more difficult for the trapped molecules to crosslink. Then they got constrained. The ramp of temperature introduced by the DSC might have turned the entire material homogeneous by rearranging the molecules of the network. That explains why we only see one Tg after.

There is no exothermic peak on the pure radical resin. Thus we are sure that this event comes only from the cationic resin.

The glass transition temperatures of the 100 wt.% radical and 100 wt.% cationic resins are identical after a photo-curing at either 20°C or at 80°C. Therefore we can assume that the curing temperature has no influence on the pure materials or that the curing temperature is too low to display any effect. It would be interesting to cure a set of samples at 150°C to validate this hypothesis.

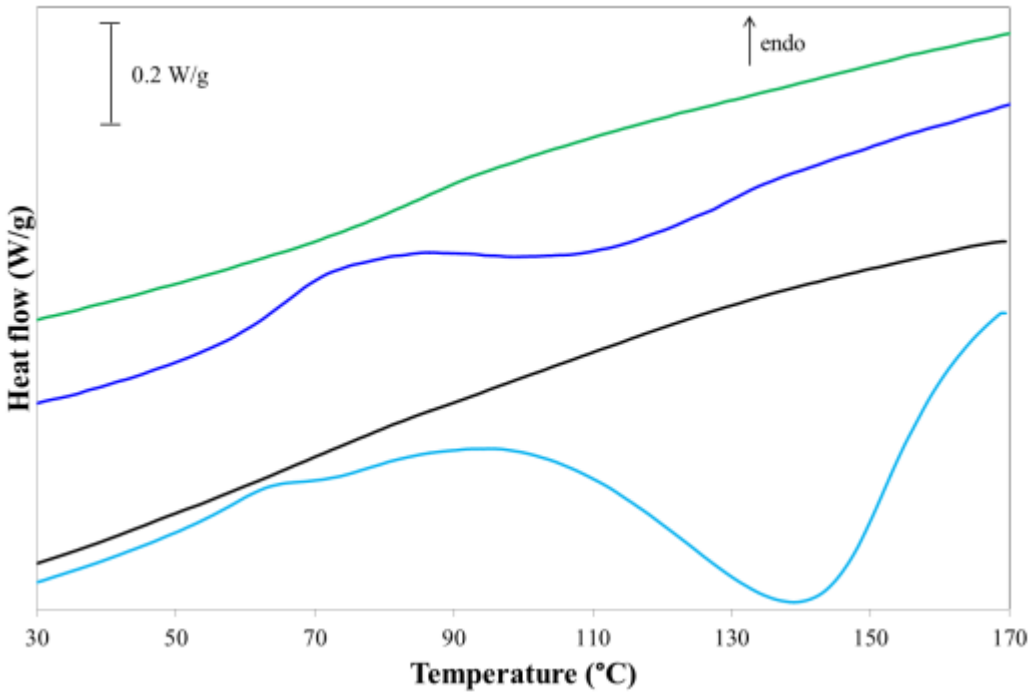

Figure 36: DSC results of a resin with proportions 25:75 wt % (radical:cationic) initiated at 20°C and 80°C - Blue (●): sample initiated at 20°C, run 1; Green (●): sample initiated at 20°C, run 2; Cyan (●): sample initiated at 80°C, run 1; Black (●): sample initiated at 80°C, run 2

The blend containing 25 wt.% radical resin has a similar behavior as the cationic resin. A heat flow step characteristic of a glass transition and an exothermic peak are observed on the first runs (Figure 36). The top of the peak is observed at 110°C for the sample prepared at 20°C and at 140°C for the sample prepared at 80°C. This shift of 30°C of this exothermic peak may be explained by the kinetics of each reaction. We

know that increasing the temperature from 25°C to 85°C can reduce the conversion time by two concerning the cationic curing [34]. So when the blends are cured at 80°C, cationic reaction occurs simultaneously with the radical one. At 20°C, the radical curing occurs first. The viscosity is then increased and the mobility decreased in the bulk while the cationic reaction is has just begun. Thus the curing is stopped earlier.

When processed at ambient temperature, the second run of the blend shows one clear Tg, the other one is not clearly identified. We can slightly observe two Tg on the second scan of the sample cured at 80°C (appendix B).

The sample cured at 80°C shows an enthalpy of curing (depth of the peak) higher than the one cured at room temperature. That may be explained as follows: when cured at 20°C, a certain amount of cationic resin was stuck in the radical network formed. This hypothesis involved that the cationic initiators will not diffuse in this area. This uncured material would remain trapped in the network and may be unable to cure despite the increase of temperature. Mechanical tests could help to understand this and check if the cationic network either was formed or still remains uncured. In the second case, the material will only benefit properties of the radical network. Otherwise, properties can be intermediate, antagonist or synergic to the ones of separate polymers.

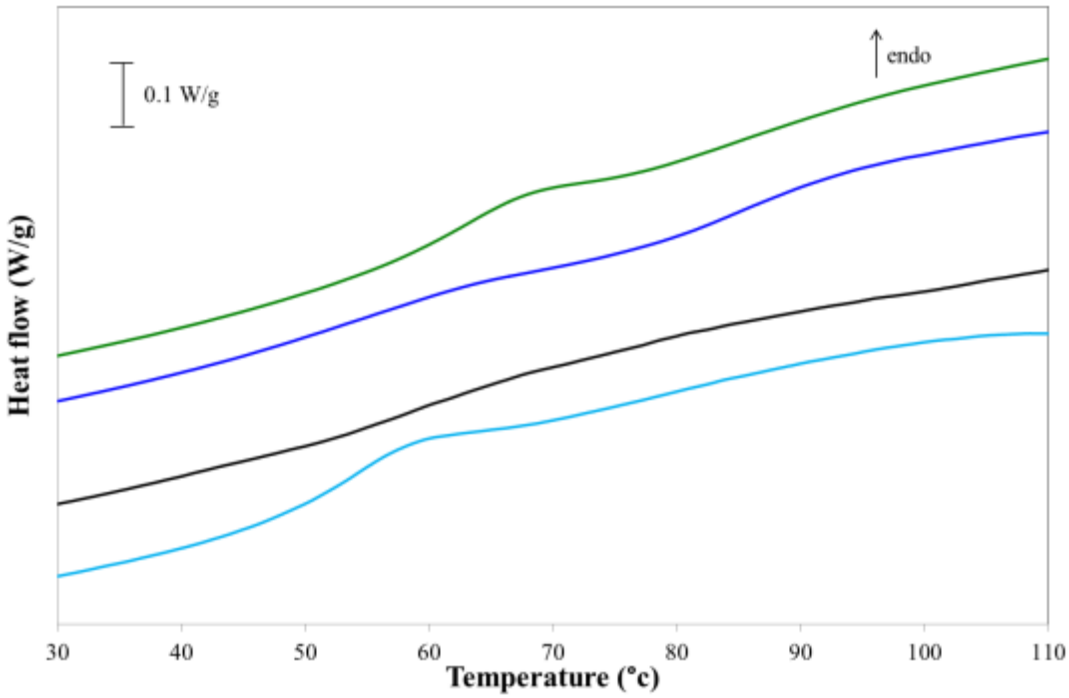

Figure 37: DSC results of a resin with proportions 40:60 wt. % (radical:cationic) initiated at 20°C and 80°C - Blue (●): sample initiated at 20°C, run 1; Green (●): sample initiated at 20°C, run 2; Cyan (●): sample initiated at 80°C, run 1; Black (●): sample initiated at 80°C, run 2

The exothermic peaks detected previously are not as obvious with the specimens containing 40 wt.% radical (Figure 37). When the blend is made at ambient temperature, we can see two glass transitions. From the first to the second scan, the first characteristic temperature, which we can match to the radical network glass transition, is increased by 5°C. This can correspond to a rearrangement of the network and then a homogenization of Tg.

On the second scan of the sample cured at 80°C, the second Tg (i.e. the glass transition assigned to the relaxation of the cationic network) is more difficult to observe, the ΔCp is two times weaker than for the sample processed at ambient temperature. This low ΔCp is characteristic of a low mobility and means that the chains are more organized.

Thus the network is less able to move during the relaxation and the Tg is less visible. This matches with the idea of the network undergoing a thermal post-curing.

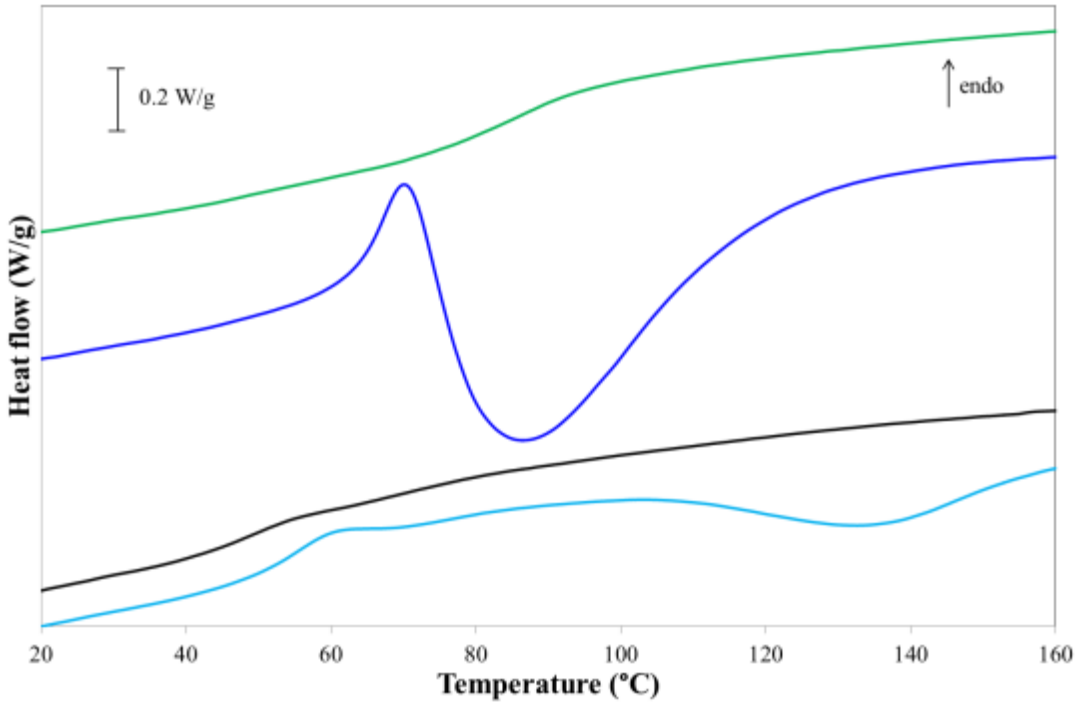

Figure 38: DSC results of a resin with proportions 50:50 wt. % (radical:cationic) initiated at 20°C and 80°C - Blue (●): sample initiated at 20°C, run 1; Green (●): sample initiated at 20°C, run 2; Cyan (●): sample initiated at 80°C, run 1; Black (●): sample initiated at 80°C, run 2

We clearly can see the signatures of the cationic network in the analysis of the blend containing 50 wt.% radical. The first run shows an exothermic peak characteristic of the thermal post-curing, which is weaker (from 30 J/g to 5.8 J/g) and shifted towards higher temperature (from 85°C to 135°C) when the sample is cured at 80°C. It is shown on Figure 38. This result is expected since the sample cured at 80°C should have benefited of a better mobility and then a higher degree of conversion of reacting species. Surprisingly, we didn't see this phenomenon on the sample containing 25 wt.% radical.

Concerning the blend made at ambient temperature, we can detect only one Tg on the first scan. It seems that the exothermic peak is hiding the cationic Tg. On its second scan, only one endothermic step is clearly observable. It is difficult to decide which network to make it match to. According to the Tg of the pure radical resin on the same analysis (68°C), we should assign it to the cationic network. But the ΔTg is spread out on 50°C. But from the previous blend (40 wt. % radical), the radical and the cationic glass transitions are about 20°C widespread each. So that means that the two Tg of both networks might be contained in one on the second run of the 50 wt. % radical sample cured at 20°C .

Two Tg were identified on the second scan of the material processed at 80°C (Appendix B), even though the second one is roughly seeable. This can be explained by a high degree of curing justified by the weak curing peak on the first scan.

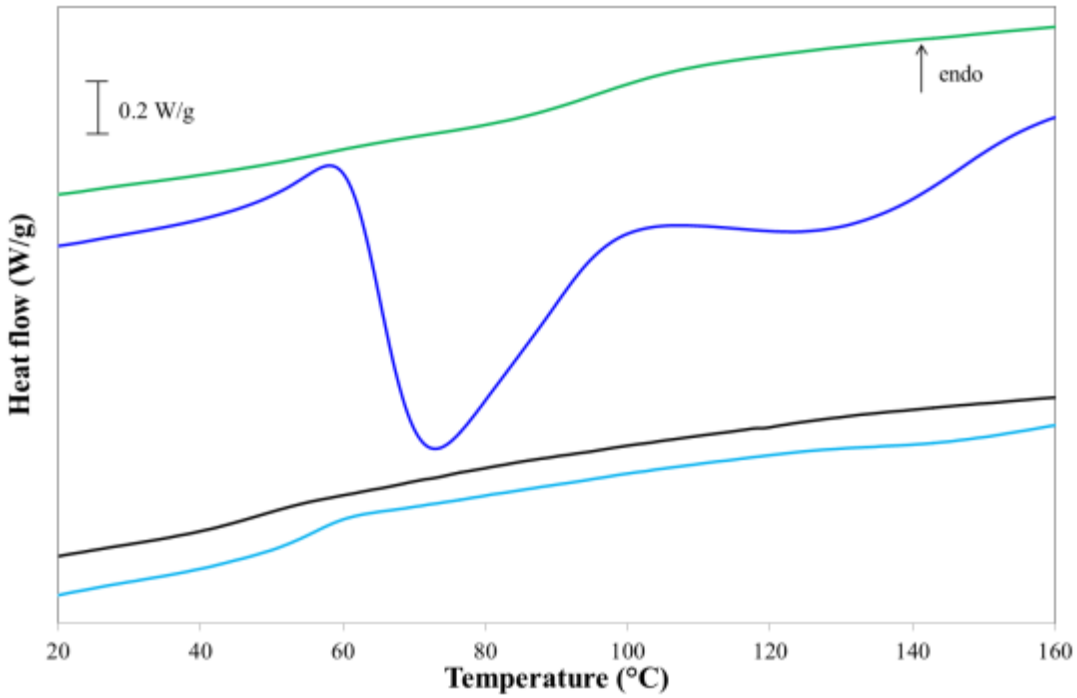

Figure 39: DSC results of a resin with proportions 60:40 wt. % (radical:cationic) initiated at 20°C and 80°C - Blue (●): sample initiated at 20°C, run 1; Green (●): sample initiated at 20°C, run 2; Cyan (●): sample initiated at 80°C, run 1; Black (●): sample initiated at 80°C, run 2

The blend containing 60 wt.% radical are shown on Figure 39. When the material was cured at room temperature, it behaves like the 50 wt.% radical blend. We see a wide curing peak on the first run, with a high enthalpy (57 J/g). But this peak is divided into two parts. The second run shows two Tg but the first one, which is characteristic of the radical network relaxation, has a ΔCp of 0.03 $J.g^{-1}.K^{-1}$ and is barely visible.

For the resin cured at high temperature, we see two Tg on the first run, but the second one, which is characteristic of the cationic network relaxation, is very narrow (ΔCp = 0.04 $J.g^{-1}.K^{-1}$). As the post-cure is also barely visible, we don't see this step on the second run anymore.

It doesn't seem that there is any obvious relationship between ΔCp and temperature or contents ratios. These systems may involve lots of interactions between the two networks. Then an accurate analysis of thermal behavior turns out very complex.

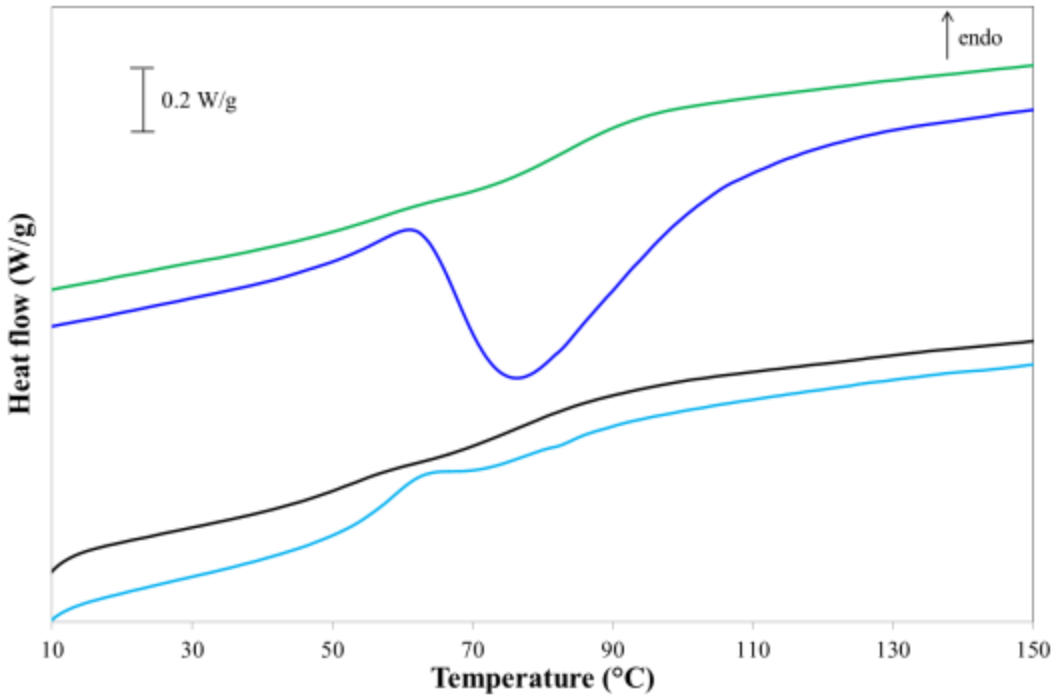

Figure 40: DSC results of a resin with proportions 75:25 wt. % (radical:cationic) initiated at 20°C and 80°C - Blue (●): sample initiated at 20°C, run 1; Green (●): sample initiated at 20°C, run 2; Cyan (●): sample initiated at 80°C, run 1; Black (●): sample initiated at 80°C, run 2

The Figure 40 shows the analyses of the blends with 75 wt.% radical. This blend has a similar behavior as the one with 60 wt% radical resin. The first run of the blend processed at ambient temperature has a deep curing peak with a ΔH of 17 J/g. From the first run of the sample cured at 80°C, we can deduce a thermal post-curing from a slight deformation of the baseline during the end of the glass transition of the radical network.

Both second runs contain two Tg located at the same place with a higher ΔCp for the cationic network. In this case, the process temperature doesn't seem to have any influence on the post cured materials.

Concerning the blends cured at 20°C, a particular behavior is observed on the first scans. Except for the 40 wt% radical, it turns out that the Tg we can measure is defined by the major network in terms of weight. This is related to the difficulty to detect a low mass signal and also that the creation of the predominant network (in terms of weight) may prevent the creation of the other network.

Concerning the samples cured at 80°C, the analysis of the thermodynamic parameters of the different materials is even more complex. One can assume that this complex behavior is directly related to the increase of interactions between the two networks, this increase being allowed by the increase of temperature (from 20°C to 80°C) which leads to a better diffusion of reactive species.

Table 4 and Table 5 are presented below with the different glass transition temperatures and their associated ΔCp. Tg_{rad} and $Tg_{rad'}$ are the glass transition temperatures associated to the radical network. Tg_{cat} is the glass transition temperature associated to the cationic network. ΔCp_{rad} and $\Delta Cp_{rad'}$ corresponds to the variation of Cp between before and after the glass transition of the radical network. ΔCp_{cat} corresponds to the variation of Cp between before and after the glass transition of the cationic network.

Table 4: Thermodynamic parameters related to the glass transition of pure and blended resins cured at 20°C after two identical scans

	Run 1						Run 2			
% Radical	Tg_{rad} (°C)	Tg_{rad}' (°C)	Tg_{cat} (°C)	ΔCp_{rad} J/(g.K)	$\Delta Cp_{rad}'$ J/g.K)	ΔCp_{cat} J/(g.K)	Tg_{rad} (°C)	Tg_{cat} (°C)	ΔCp_{rad} J/(g.K)	ΔCp_{cat} J/(g.K)
0			63			0.13		115		0.2
25			64			0.06		85		0.05
40	53		85	0.05		0.07	58	86	0.13	0.07
50	55			0.41				81		0.16
60	54			0.13			55	95	0.03	0.17
75	55			0.06			52	85	0.027	0.18
100	46	72		0.09	0.12		68		0.26	

Table 5: Thermodynamic parameters related to the glass transition of pure and blended resins cured at 80°C after two identical scans

	Run 1						Run 2					
% Rad	Tg_{rad} (°C)	Tg_{rad}' (°C)	Tg_{cat} (°C)	ΔCp_{rad} J/(g.K)	$\Delta Cp_{rad}'$ J/(g.K)	ΔCp_{cat} J/(g.K)	Tg_{rad} (°C)	$Tg_{rad'}$ (°C)	Tg_{cat} (°C)	ΔCp_{rad} J/(g.K)	$\Delta Cp_{rad'}$ J/(g.K)	ΔCp_{cat} J/(g.K)
0			63			0.11			115			0.15
25	56			0.05				71	115		0.03	0.05
40	52		85	0.09		0.12	58		113	0.04		0.03
50	54		80	0.12		0.08	45	74		0.08	0.03	
60	52		106	0.15		0.04	47			0.05		
75	56		94	0.14		0.22	50	78		0.04	0.15	
100	46	76		0.04	0.15			68			0.24	

3.2.5 Discussion

Many blended materials were designed with different components, ratios and process temperatures from two different curing mechanisms. We first had to find a good set of components. It was noticed that solid initiators don't dissolve very good in the mixture. We also needed to find components that cure pretty fast in order to respect the goal of the project in which our work is inscribed. Using different analysis technics helped us to understand both pure and mixed resins behaviors. Since the systems are very complex, it was decided to work only with crosslinkers. Using monomer, or plasticizer, was dropped.

It is well known from the literature that photo-cured cationic systems don't end up to a fully cured material. A thermal post-cure is able to increase their crosslinking rates though. FTIR spectroscopy informed us about the influence of the process temperature on the cationic system we used. It turns out that processing the pure cationic resin at high temperature increased a lot the curing rate, from 55 % to 92 %. We should expect roughly the same behavior when the resin is blended with some radical compound but the quality of the signals are very bad since the spectrum of the radical resin interferes within the region of interest.

DSC analyses gave us information about thermal properties of our materials. The Figure 41 and the Figure 42 are showing the evolution of the Tg of radical and cationic resins for the samples cured at 20°C during the first and the second scan respectively. It seems that glass transition temperatures of both components stay stable within the range

of concentration. The radical Tg is around 60°C on the two scans. We can assume that the degree of conversion of the radical part was around 60-80 % [32] at least in the bulk considering the high viscosity of the different systems. The cationic Tg doesn't look to be influenced by the concentration either, but increased on the second run. That makes sense regarding to the curing peak observed on the DSC and also regarding to the degree of conversion of only 55 % for the cationic resin using the FTIR. Moreover, we deduce that we can post-cure the blend materials to increase the cationic degree of conversion without altering the radical chains. The behavior of one component can be described as independent from the other's one. This is a first clue rejecting the possibility to have Interpenetrating Polymer Networks.

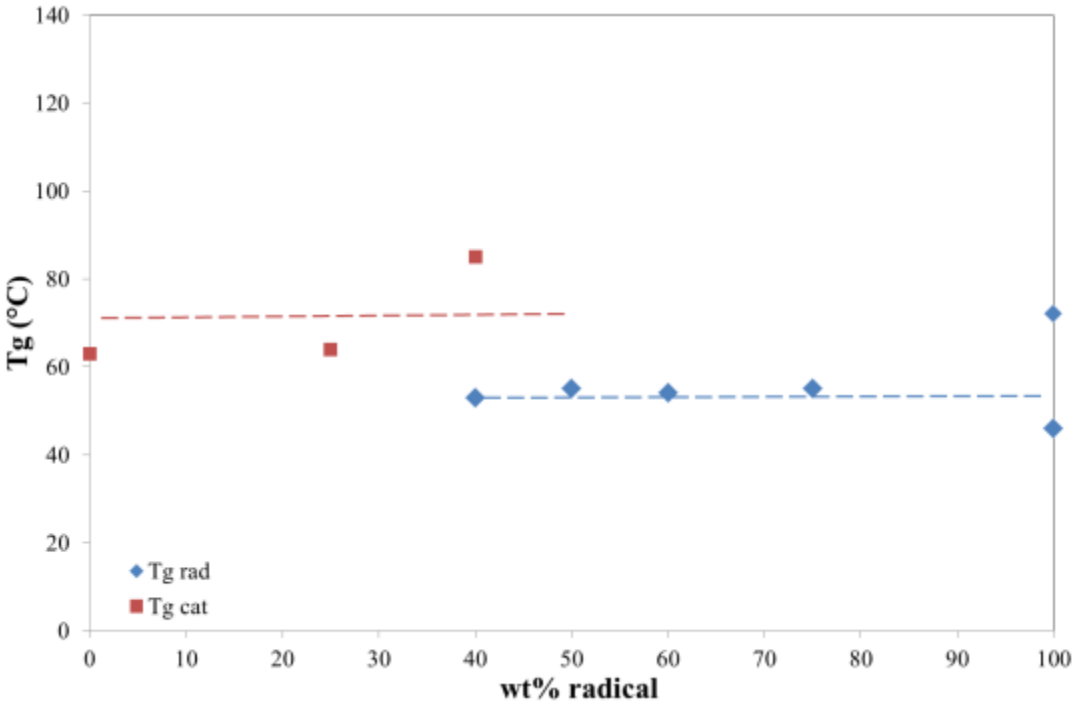

Figure 41: Evolution of the glass transition temperature vs. wt% radical resin cured at 20°C – scan 1

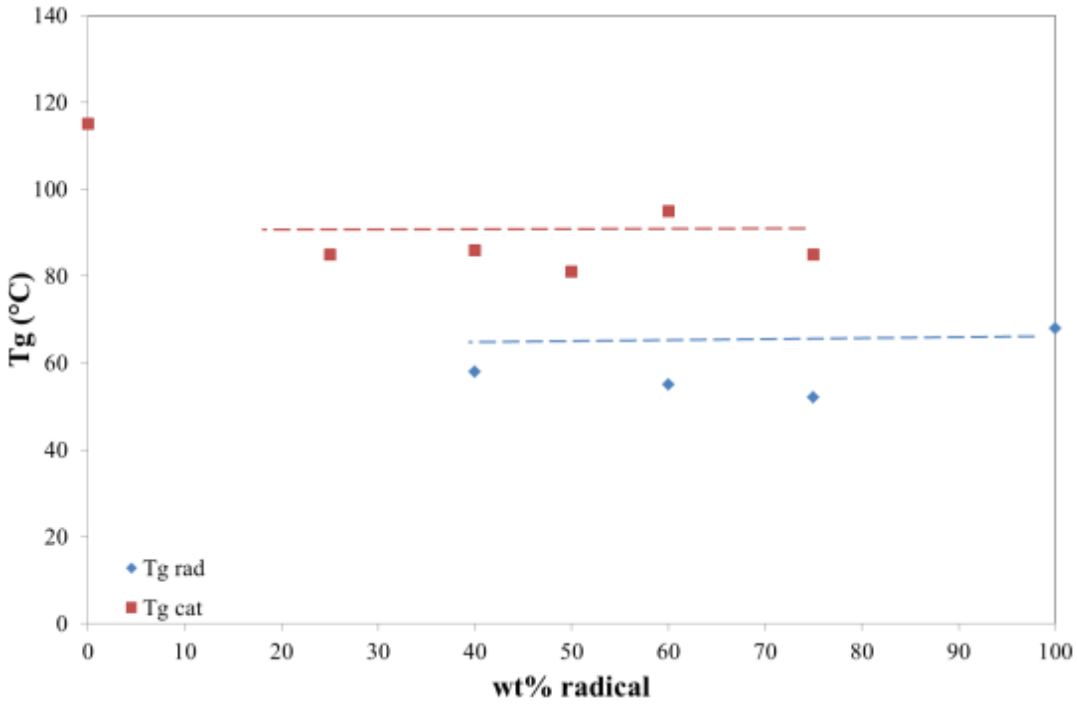

Figure 42: Evolution of the glass transition temperature vs. wt% radical resin cured at 20°C – scan 2

Concerning the resins initiated at 80°C, we can clearly notice diffusion changes between the two networks (Figure 43). On the first run, the radical part has the same properties as when it was cured at 20°C. But the Tg of the cationic material is higher, except for the pure cationic. It is higher and higher as the ratio of radical is higher. Actually, we saw earlier that increasing the temperature can reduce the conversion time of the cationic network by two [34]. So blends cured at 80°C allow a more simultaneous curing reaction of the radical and cationic systems. Therefore the cationic curing can go further and reach a higher Tg with the higher mobility. Its Tg would go even higher with increasing the amount of radical resin because this last one is less viscous at high temperature and increases the mobility of the solution.

The two networks described singularly different thermal behaviors during the second scan. It seems that resins have much more interactions on each other after post-cure. According to the Figure 44, the Tg of the cationic resin is around 115°C like the pure material. But we were able to detect it only up to 40 wt.% radical. Compared to the first run, we clearly see that a post-cure occurred though. The absence of signature of the cationic network above a weight proportion of 40 % in radical content can be explained by two different ways. Either the high content of radical compound holds the cationic part and avoids it to relax at its glass transition; or the mass of cationic part starts to be too low compared to the one of the radical part. In that case, it might be too difficult for the cationic signature to be detected or there may be a dilution effect that decreases the reaction rate and increases the curing time needed to complete the cure.

Concerning the radical network, it shows two signatures of glass transition in the blends from 40 wt.% to 75 wt.% radical like the pure radical before post-cure. After post-cure, we assume that the entire radical network didn't succeed to rearrange and increase its Tg. So some part got fully formed and some other part could have been stuck. By the way, this behavior is confirmed by the results obtained by AFM on the pure radical resin. These two different kind of phases may be related to the two signatures of glass transition measured by DSC. In that case, the control of thermal post-cure is essential for other analyses and optimal conditions of use. It seems obvious that a material with 2 Tg should have different mechanical properties than a material with an homogeneous Tg.

Moreover, it was reported that cationic and radical resins have an antagonist behavior with increasing the temperature [35]. Although the curing rate of the cationic resin

strongly increases, the radical resin gets a decrease of its curing rate and then an increase of its curing time.

All these signatures are characteristic of multiple demixing and show that temperature control is not enough to get an IPN.

DSC alone is not enough to find the origin of this phenomenon. We can suggest a hypothesis though. The increase of temperature has been accompanied by an increase of chain mobility leading to a highest number of interactions between the two networks. It results from this that the thermodynamic behaviour of each system becomes significantly more complex.

We suggest that Dynamic Mechanical Analysis would be useful to get a better understanding of the materials behaviors.

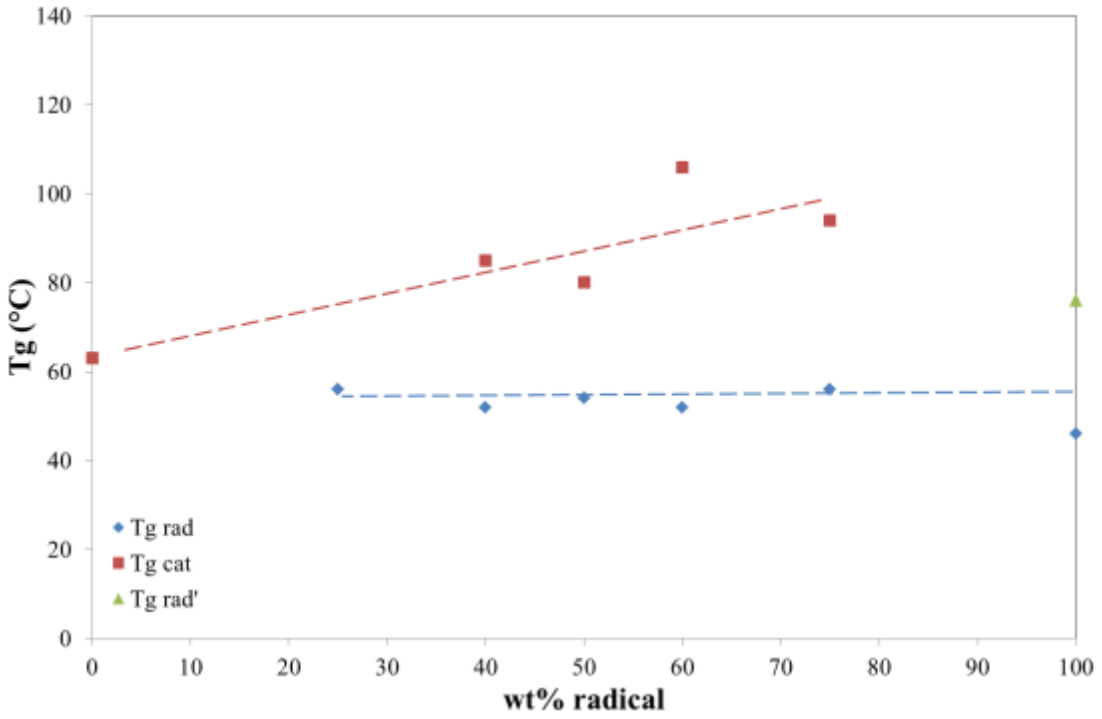

Figure 43: Evolution of the glass transition temperature vs. wt% radical resin cured at 80°C – scan 1

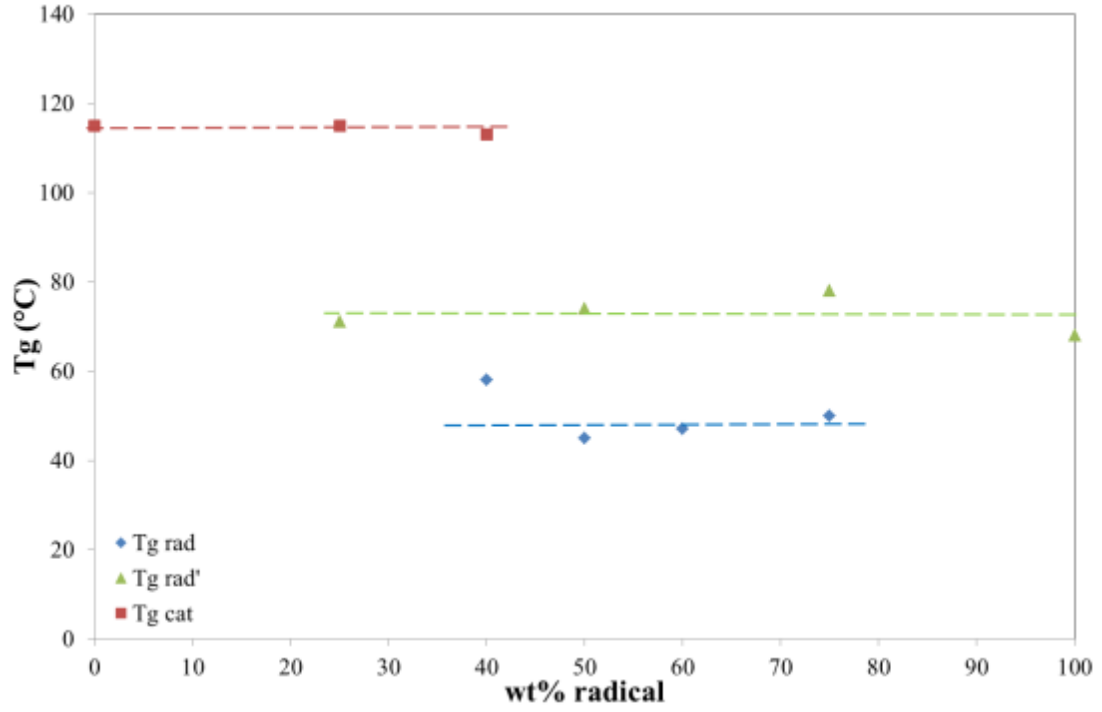

Figure 44: Evolution of the glass transition temperature vs. wt.% radical resin cured at 80°C – scan 2

These data are complementary to each other and helped us to understand how the cationic and the radical resins behave after photo-curing separately and blended with different proportions. The fact of using two different curing mechanisms needed to adapt the process in order to satisfy both reactions. The radical reaction was bothered by oxygen and the cationic one by humidity. They also have two different kinetics. We noticed that the radical curing, which is the faster, is influenced by the cationic system. This last one forms its own network independently of the radical resin content. Properties of the radical network and then the entire material will be managed by the bulk temperature and the proportions between the two components. Although, the influence of proportions doesn't describe a linear polymer blends law, presence of IPN is not proved though. Additional technics would be welcomed to answer this question because signals of the two materials are disturbing each other with FTIR. Also, the thermal properties of both networks are very close and sometimes difficult to distinguish. We worked with high speed DSC to detect them. In this way, the sensibility is improved to the detriment of the resolution. It is justified by the fact that the mobility of thermosets is not very sensitive to heat. But since the two Tg are so close, a better resolution would be appreciated. Anyway, this doesn't alter the fulfillment of our objective. The TGA showed that we got homogenous blends even though the radical resin was heterogeneous itself. It also showed that blends were not undergoing linear degradation process in function of radical content. It was noticed that different properties were obtained within these blends depending on the proportions and the process temperature.

Chapter 4

Summary and Conclusion

Materials design sometimes needs to satisfy complex requirements. Competent domains like sport, automotive, aeronautics, electronics or military are developing various properties materials that need to be put together. But there are some issues with assembling several elements together. The cost of process is increased and interfaces may be birth of cracks. Final properties and life time of materials are then reduced.

Our research work consisted in one hand to check the miscibility of two thermosetting polymers using two different mechanisms of reaction. Radical curing and cationic curing were used. These two reactions are occurring with different kinetics and different thermodynamics. The radical system is formed very fast from free radicals initiation but is inhibited by presence of oxygen. It leads to high degree of conversion. The cationic system is formed from oxirane ring opening and is inhibited by presence of humidity. It needs post-thermal curing to optimize its curing rate. Free radicals are released during the initiation of the cationic system and contribute to the radical reaction. To put this factor away, both systems were initiated simultaneously. Fine chemistry conditions ended up to macroscopically stable materials. This has been verified by TGA (Thermogravimetric Analysis) all over a range of ratios between radical and cationic crosslinkers.

On a second hand, influence of the networks on each other was studied using DSC (Differential Scanning Calorimetry). For this, samples with 0 wt.%, 25 wt.%, 40 wt.%, 50 wt.%, 60 wt.%, 75 wt.%, 100 wt.% radical compound were analyzed. As a result, we saw that mixing the two systems at room temperature had no influence on thermal properties of each network. Tapping mode of AFM (Atomic Force Microscopy) was used as a morphologic analysis. Different phases were observed but it would be necessary to determine a degree of phase separation. The two systems might be not crosslinked since no strong interaction are detected.

FTIR (Fourier Transform Infrared) spectrometry showed that the cationic system had a very low conversion rate at ambient temperature. One noticed that this degree of conversion was much higher at 80°C. A different technic would be welcomed to check if this is verified in blends.

On another hand, DSC analysis were carried out on blended samples processed at 80°C to investigate an influence of process temperature on the final result. Interactions between the two networks were noticed with a modification of thermal properties. DSC curves showed smaller ΔCp than the ones of samples prepared at 20°C. Glass transitions of both networks were very narrow and roughly detectable. One deduced that the microstructure was better organized. A morphologic analysis would certainly show small phase domains.

Within future works, one should work with systems which are even more different in terms of properties in order to enlarge the investigation field in terms of thermo-

mechanical properties. In particular, we can expect that working with crosslinkers exhibiting a wide difference of glass transition temperature will allow obtaining a wider range of potential properties. This could be done for example by choosing a long chain crosslinker leading after UV-curing to a soft material. Since the process was adapted to create well organized networks, which have a very low molecular mobility, one reached the limit of sensibility of the DSC used to properly detect their thermal properties. Other available technics like DMA (Dynamic Mechanical Analysis) would be more adapted though. Finally this work has evidenced the crucial role of reactive species mobility to obtain high degree of conversion. Different ways can be considered to push forward this effect as increasing the process temperature, working with solvated crosslinker or even decreasing the bulk viscosity by adding monomers.

Appendix A: additional tables of experiments

Sample #	Radical (weight in g)			Cationic (weight in g)		Atmosphere & UV exposure (sec)	Aspect
	Crosslinker	Monomer	Photo-initiator	Crosslinker	Photo-initiator		
	Bisphenol A propoxylate diacrylate	2-Ethylhexyl acrylate	Phenylbis(2,4,6-trimethylbenzoyl) phosphine oxide	1,4-cyclohexanedimethanol diglycidyl ether	Triarylsulfonium hexafluoroantimonate salts		
1	0.48	1	0.001	0	0	O_2 - 10	Sticky
2	0.48	1	0.001	0	0	N_2 - 10	Brittle
3	0	0	0	1	0.02	O_2 - 10	Hard
4	0	0	0	1	0.02	N_2 - 10	Hard
5	0.48	1	0.001	1	0.02	N_2 - 10	Brittle
6	1	0	0.02	0	0	$N_2 - 900$	Hard, yellow
7	1	0	0.02	0	0	$N_2 - 120$	
8	1	0	0.02	0	0	$N_2 - 60$	
9	1	0	0.02	0	0	$N_2 - 30$	
10	1	0	0.02	0	0	N_2 - 5	
11	1	0.5	0.05	0	0	N_2 - 5	Brittle
12	0	0	0	1	0.07	$N_2 - 30$	Hard, brown
13	0	0	0	1	0.07	$N_2 - 30$	

Table 6: Experiments realized with the systems crosslinker + monomer

Sample #	Radical (weight in g)			Cationic (weight in g)		Atmosphere & UV exposure (sec)	Decision
	Crosslinker	Monomer	Photo-initiator	Crosslinker	Photo-initiator		
	Bisphenol A propoxylate diacrylate	2-Ethylhexyl acrylate	Phenylbis(2,4,6-trimethylbenzoyl) phosphine oxide	1,4-cyclohexanedimethanol diglycidyl ether	Triarylsulfonium hexafluoroantimonate salts		
1	0.48	1	0.001	0	0	O_2 - 30	Sticky
2	0.48	1	0.001	0	0	N_2 - 30	Brittle
3	0	0	0	1	0.02	O_2 - 10	Hard
4	0	0	0	1	0.02	N_2 - 10	Hard
5	0.48	1	0.001	1	0.02	N_2 - 10	Brittle
	0.12	1	0.001	0	0	N_2 - 10	Sticky
	0.06	1	0.0001	0	0	N_2 - 10	
	0.03	1	0.0001	0	0	N_2 - 10	
	0.6	1	0.001	0	0	N_2 - 10	
	0.7	1	0.001	0	0	N_2 - 10	
	0.84	1	0.001	0	0	N_2 - 10	
	0.6	1	0.001	0	0	N_2-10-thin layer	Hard, yellow
	0.49	1	0.001	0	0	N_2-300-thin layer	
	0.86	1	0.001	0	0	N_2-300-thin layer	
10	1	0	0.02	0	0	N_2 - 5	Brittle, soft
11	1	0.5	0.05	0	0	N2 – 30	Hard, brittle, brown
12	0	0	0	1	0.07		
	0	0	0	1	0.08	N2 – 30 Sonication	
13	0	0	0	1	0.07		

Table 7: Experiments of system "crosslinker+monomer" realized with Phenylbis(2,4,6-trimethylbenzoyl) phosphine oxide as photo-initiator

Sample #	Radical (weight in g)			Cationic (weight in g)		Atmosphere & UV exposure (sec)	Decision
	Crosslinker	Monomer	Photo-initiator	Crosslinker	Photo-initiator		
	Bisphenol A propoxylate diacrylate	2-Ethylhexyl acrylate	2-hydroxy 2-methyl propiophenone	1,4-cyclohexanedimethanol diglycidyl ether	Triarylsulfonium hexafluoroantimonate salts		
14	1	0.5	0.02	0	0		
	1.3	0.1	0.015	0	0	N_2-30	Hard, cured
	1.15	0.2	0.015	0	0	N_2-30	
	1	0.3	0.015	0	0	N_2-30	
	3	0	0.015	0	0	N_2-30	
	2.8	0.35	0.015	0	0	N_2-30	
	2	0.8	0.015	0	0	N_2-30	
	1.4	1.7	0.015	0	0	N_2-30	
	0	3	0.015	0	0	N_2-30	
	2.5	0	0.015	0	0	N_2-30	Accepted
	2.5	0.32	0.015	0	0	N_2-30	Accepted
	2.5	1	0.015	0	0	N_2-30	Accepted
	2.5	3.1	0.015	0	0	N_2-30	Accepted
	0	3	0.015	0	0	N_2-30	Accepted
	1.5	0	0.015	1.5	0.015	N_2-30	Accepted
	1.5	0	0.015	1.5	0.015	N_2-30	Accepted
	1.5	0	0.015	1.5	0.015	N_2-30	Accepted
	1.5	0	0.015	1.5	0.015	N_2-30	Accepted
	1.5	0.4	0.015	0.9	0.015	N_2-300	
	1.5	0	0.015	1.5	0.015	N_2-300	

Table 8: Experiments of system "crosslinker+monomer" realized with 2-hydroxy 2-methyl propiophenone as photo-initiator

Radical (weight in g)			Cationic (weight in g)		Atmosphere & UV exposure (sec)	Decision
Crosslinker	Monomer	Photo-initiator	Crosslinker	Photo-initiator		
Bisphenol A propoxylate diacrylate	2-Ethylhexyl acrylate	AIBN	1,4-cyclohexanedimethanol diglycidyl ether	Triarylsulfonium hexafluoroantimonate salts		
0.48	1	0.001	0	0	80°C N_2	
0.48	1	0.003	0	0	80°C N_2	
0.43	1	0.0015	0	0	80°C N_2	
0.67	1	0.0015	0	0	80°C N_2	
1.5	1	0.0015	0	0	80°C N_2	
1	0	0.01	0	0	80°C N_2	
1	0	0.006	0	0	80°C N_2	Hard, cracks
1	0	0.025	0	0	80°C N_2	
1	0.1	0.012	0	0	80°C N_2	
1	0.2	0.012	0	0	80°C N_2	
1	0.3	0.012	0	0	80°C N_2	
1	0.5	0.03	0	0	80°C N_2	
1	0.9	0.03	0	0	80°C N_2	
1	1.3	0.04	0	0	80°C N_2	
1	1.7	0.05	0	0	80°C N_2	
1	2.1	0.06	0	0	80°C N_2	

Table 9: Experiments of system "crosslinker+monomer" realized with AIBN as thermal initiator

Rad/Cat crosslinkers ratio (wt. %)	Radical (weight in g)		Cationic (weight in g)		Atmosphere & UV exposure (sec)	Decision
	Crosslinker	Photo-initiator	Crosslinker	Photo-initiator		
	Bisphenol A propoxylate diacrylate	2-hydroxy 2-methyl propiophenone	3,4 epoxycyclohexylmethyl 3,4 epoxycyclohexane carboxylate	Triarylsulfonium hexafluoroantimonate salts		
25/75	0.75	0.015	2.25	0.015	N_2+O_2 - 20°C	Rejected
25/75	0.75	0.015	2.25	0.015	N_2+O_2 - 20°C	Rejected
50/50	1.5	0.015	1.5	0.015	N_2+O_2 - 20°C	Rejected
50/50	1.5	0.015	1.5	0.015	N_2+O_2 - 20°C	Rejected
75/25	2.25	0.015	0.75	0.015	N_2+O_2 - 20°C	Rejected
75/25	2.25	0.015	0.75	0.015	N_2+O_2 - 20°C	Rejected
0/100	0	0.018	3	0.018	N_2 - 20°C	Accepted
15/85	0.45	0.018	2.55	0.017	N_2 - 20°C	Accepted
25/75	0.75	0.015	2.25	0.018	N_2 - 20°C	Accepted
32/68	1.02	0.017	1.98	0.019	N_2 - 20°C	Accepted
40/60	1.2	0.016	1.8	0.016	N_2 - 20°C	Accepted
45/55	1.35	0.019	1.65	0.019	N_2 - 20°C	Accepted
50/50	1.5	0.014	1.5	0.013	N_2 - 20°C	Accepted
60/40	1.8	0.012	1.2	0.013	N_2 - 20°C	Accepted
75/25	2.25	0.015	0.75	0.019	N_2 - 20°C	Accepted
100/0	3	0.015	0	0	N_2 - 20°C	Accepted
0/100	0	0	3	0.06	N_2 - 80°C	Accepted
25/75	0.75	0.0015	2.25	0.045	N_2 - 80°C	Accepted
40/60	1.2	0.0024	1.8	0.036	N_2 - 80°C	Accepted
50/50	1.5	0.003	1.5	0.03	N_2 - 80°C	Accepted
60/40	1.8	0.0036	1.2	0.024	N_2 - 80°C	Accepted
75/25	2.25	0.0045	0.75	0.015	N_2 - 80°C	Accepted
100/0	3	0.006	0	0	N_2 - 80°C	Accepted

Table 10: Experiments of system "crosslinker only" realized with 2-hydroxy 2-methyl propiophenone as photo-initiator

Appendix B: Zoom of DSC curves

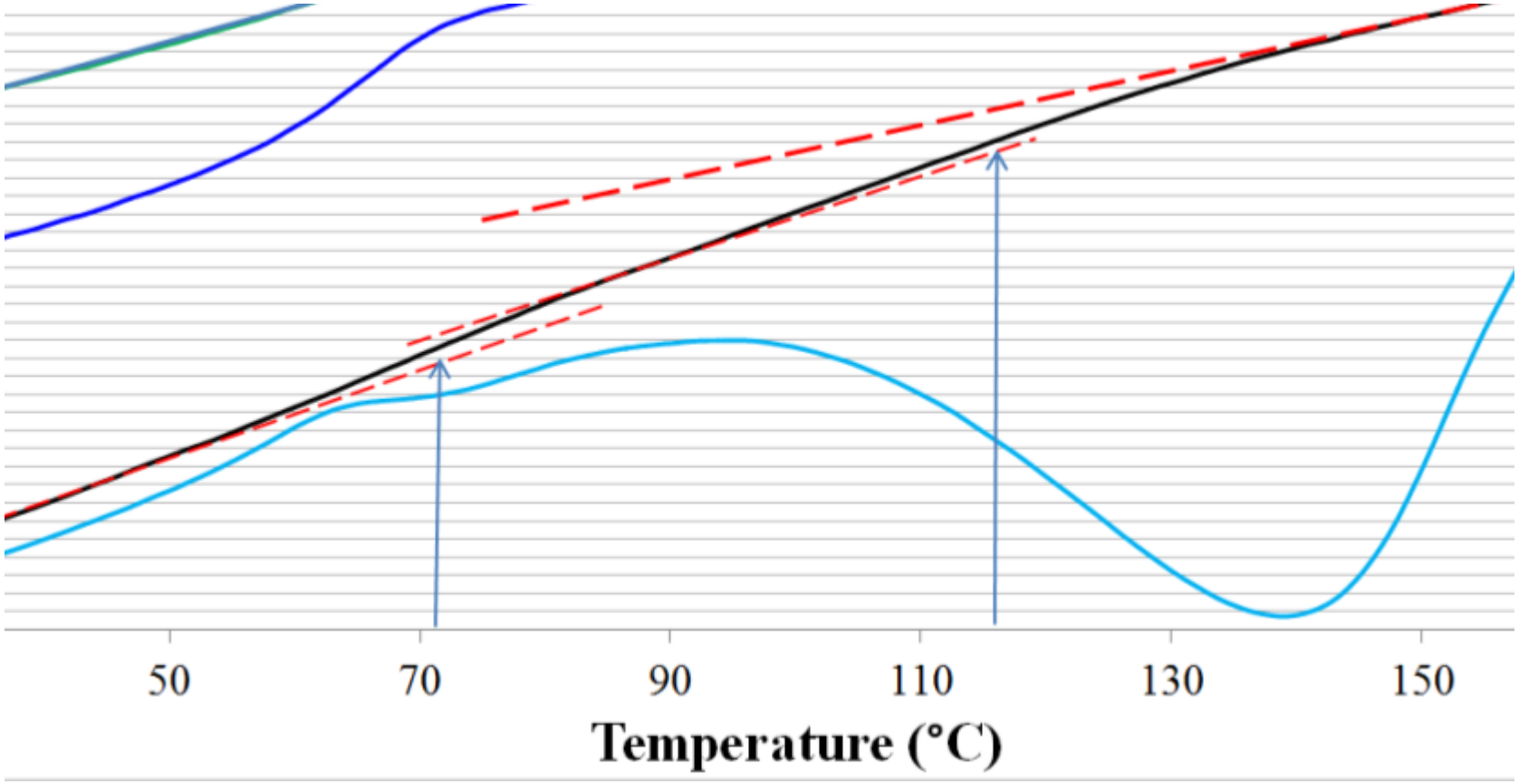

Figure 45: Zoom of the DSC results of a resin with proportions 25:75 wt % (radical:cationic) initiated at 80°C. (Black (●)): sample initiated at 80°C, run 2

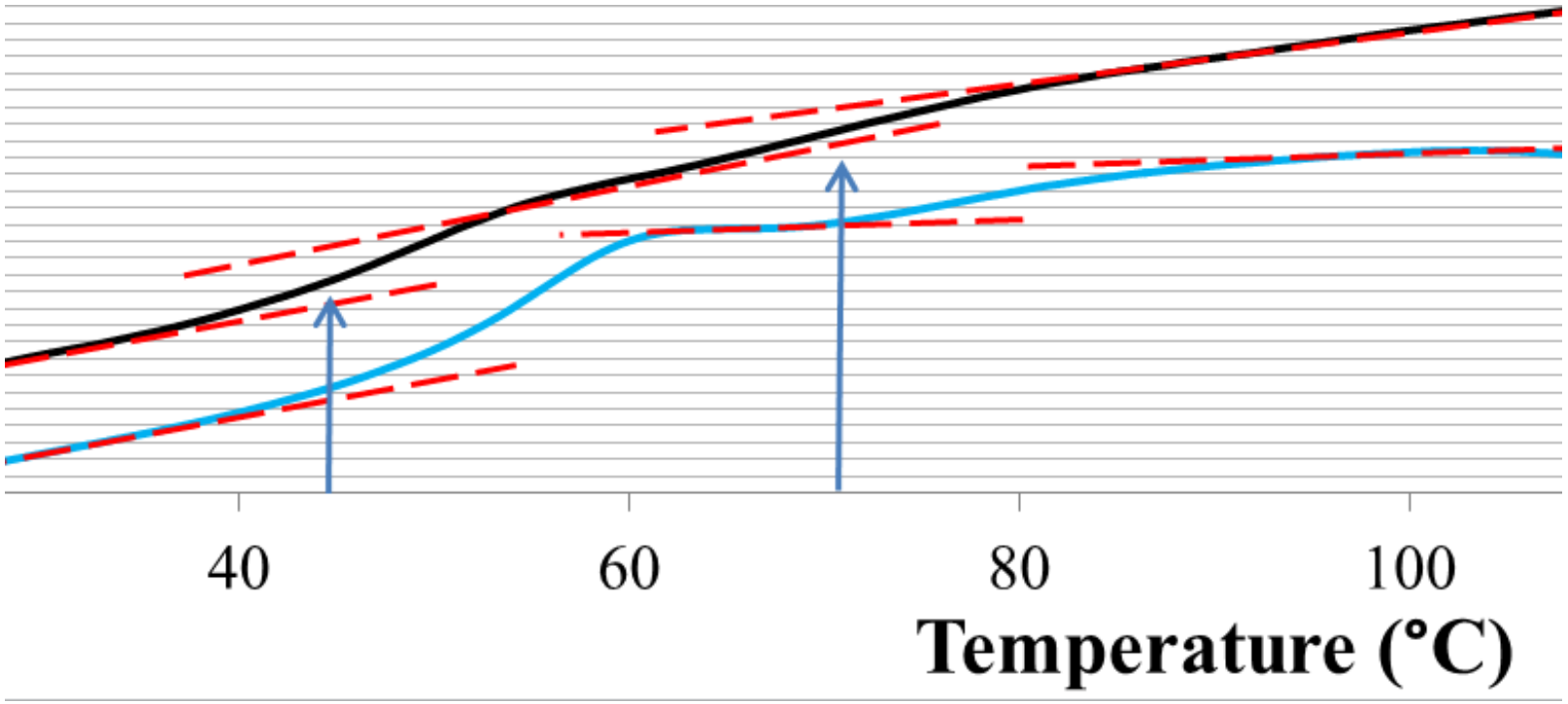

Figure 46: Zoom of the DSC results of a resin with proportions 50:50 wt. % (radical:cationic) initiated at 20°C and 80°C . Black (●): sample initiated at 80°C, run 2

References

[1] Ranade, S. V., Richard, R. E., Helmus, M. N., *Styrenic block copolymers for biomaterial and drug delivery applications*, Acta Biomateriala 1 (2005) 137-144

[2] Lipatov, Y. S., *Polymer blends and interpenetrating polymer networks at the interface with solids*, Progress in Polymer Science 27 (2002) 1721-1801

[3] Martin, G. C., Enssani, E., Shen, E., *Mechanical behavior of gradient polymers*, Journal of Applied Polymer Science 26 (1981) 1465-1473

[4] Vabrik, R., Czajlik, I., Túry, G., Rusznák, I., Ille, A., Víg, A., *A Study of Epoxy Resin–Acrylated Polyurethane Semi-Interpenetrating Polymer Networks*, Journal of Applied Polymer Science 68 (1997) 111-119

[5] Chen, C-H., *Interpenetrating polymer network of blocked polyurethane and phenolic resin*, Society of Plastics Engineers (2011)

[6] Desilles, N., *Nouveaux matériaux polymers à gradient de structure photoinduit : synthèse à partir d'un système liquid et etude des propriétés*, PhD thesis (2004), INSA de Rouen-France

[7] Simić, S., Dunjić, B., Tasić, S., Bozić, B., Jovanović, D., Popović, I., *Synthesis and characterization of interpenetrating polymer networks with hyperbranched polymers through thermal-UV dual curing*, Progress in Organic Coatings 63 (2008) 43-48

[8] Gonzãlez, G., Burillo, G., *Synthesis of comb type and semi-interpenetrating networks of acryloyl-L-proline methyl ester and poly(acrylicacid) for Cu(II) immobilization*, Radiation Physics and Chemistry 79 (2010) 870-875

[9] Sperling, L. H., *Interpenetrating Polymer Networks: An Overview*, American Chemical Society (1994)

[10] Gupta, N., Srivastava, A. K., *Interpenetrating Polymer Networks: A Review on Synthesis and Properties*, Polymer International 35 (1994) 109-118

[11] Akovali, G., Biliyar, K., Shen, M., *Gradient polymers by diffusion polymerization*, Journal of Applied Polymer Science 20 (1976) 2419-2427

[12] Guo, Y., Tang, D., Wang, Y., *The Influence Factors Analysiis to Improve the Compatibility and the Mechanical Behavior of IPN, Gradient IPN and $BaTiO_3$ Filled IPN*, Materials Sciences and Applications 3 (2012) 606-611

[13] Tang, D., Zhang, X., Liu, L., Qiang, L., *Simultaneous and Gradient IPN of Polyurethane/Vinyl Ester Resin: Morphology and Mechanical Properties*, Journal of Nanomaterials (2009) 514124

[14] Lipatov, YU. S., Karabanova, L. V., *Gradient interpenetrating polymer networks*, Journal of Material Science 30 (1995) 1095-1104

[15] Sperling, L. H., Manson, J. A., Oureshi, S., Fernandez, A. M., *Tough Plastics and Reinforced Elastomers from Renewable Resource Industrial Oils. A Short Review*, Industrial & Engineering Chemistry Product Research and Development 20 (1981) 163-166

[16] Désilles, N., Lecamp, L., Lebaudy, P., Bunel, C., *Elaboration of gradient structure materials from homogeneous system combining UV and thermal processes*, Polymer 45 (2004) 1439-1446

[17] Rahman, N., Khan, M. A., Khan, R. A., Chowdhury, T. A., *Modification of Gelatin Films Using Trimethylpropane Trimethacrylate (TMPTMA) by Photo-Curing*, Polymer-Plastics Technology and Engineering 50 (2011) 404-411

[18] Lecamp, L., Lebaudy, P., Youssef, B., Bunel, C., *Influence of UV radiation wavelength on conversion and temperature distribution profiles within dimethacrylate thick material during photopolymerization*, Polymer 42 (2001) 8541-8547

[19] Peterson, A. M., Kotthapalli, H., Rahmathullah, M. A. M., Palmese, G. R., *Investigation of interpenetrating polymer networks for self-healing applications*, Composites Science and Technology 72 (2012) 330-336

[20] Lecamp, L., Youssef, B., Bunel, C., Lebaudy, P., *Photoinitiated polymerization of a dimethacrylate oligomer: 1. Influence of photoinitiator concentration, temperature and light intensity*, Polymer Vol. 38 No. 25 (1997) 6089-6096

[21] Clayton, L. M., Sikder, A. K., Kumar, A., Cinke, M., Meyyappan, M., Gerasimov, T. G., Harmon, J. P., *Transparent Poly(methyl methacrylate)/Single-Walled Carbon Nanotube (PMMA/SWNT) Composite Films with Increased Dielectric Constants*, Advanced Functional Materials 15 (2005)

[22] Decker, C., Jenkins, A. D., *Kinetic Approach of O_2 Inhibition in Ultraviolet- and Laser- Induced Polymerizations*, Macromolecules 18 (1985) 1241-1244

[23] Kim, Y-M., Kostanski, L. K., MacGregor, J. F., *Photopolymerization of 3,4-epoxycyclohexylmethyl-3',4'-epoxycyclohexane carboxylate and tri(ethylene glycol) methyl vinyl ether*, Polymer 44 (2003) 5103-5109

[24] González, M. G., Cabanelas, J. C., Baselga, J., *Application of FTIR on Epoxy Resins – Identification, Monitoring the curing Process, Phase Separation and Water Uptake*, Infrared Spectroscopy – Materials Science, Engineering and Technology (2012)

[25] Esposito Corcione, C., Malucelli, G., Frigione, M., Maffezzoli, A., *UV-curable epoxy systems containing hyperbranched polymers: Kinetics investigation by photo-DSC and real-time FT-IR experiments*, Polymer Testing 28 (2009) 157-164

[26] Hsieh, K. H., Han, J. L., Yu, C. T., Fu, S. C., *Graft interpenetrating polymer networks of urethane-modified bismaleimide and epoxy (I): mechanical behavior and morphology*, Polymer 42 (2001) 2491-2500

[27] Decker, C., Nguyen Thi Viet, T., Decker, D., Weber-Koehl, E., *UV-radiation curing of acrylate/epoxide systems*, Polymer 42 (2001) 5531-5541

[28] Sangermano, M., Di Gianni, A., Bongiovanni, R., Priola, A., Voit, B., Pospiech, D., Appelhans, D., Synthesis of Fluorinated Hyperbranched Polymers and Their Use as Additives in Cationic Photopolymerization, Macromolecular Materials and Engineering 290 (2005) 721-725

[29] Lee, T. Y., Guymon, C. A., Sonny Jönsson, E., Hoyle, C. E., *The effect of monomer structure on oxygen inhibition of (meth)acrylates photopolymerization*, Polymer 45 (2004) 6155-6162

[30] SII NanoTechnology Inc., *DSC Measurements of Thermosetting Resins*, TA 8 (MAR 1981)

[31] Chartoff, R., *Thermal characteristics of thermosets formed by free radical photocuring*, Journal of Thermal Analysis and Calorimetry 85 (2006) 213-217

[32] Cheung, Y. W., Stein, R. S., *Critical Analysis of the Phase behavior of Poly(ε-caprolactone) (PCL)/Polycarbonate (PC) Blends*, Macromolecules 27 (1994) 2512-2519

[33] Crivello, J. V., Lam, J. H. W., *The Photoinitiated Cationic Polymerization of Epoxy Resins*, Epoxy Resin Chemistry (1979)

[34] Nowers, J. R., Narasimhan, B., *The effect of interpenetrating polymer network formation on polymerization kinetics in an epoxy-acrylate system*, Polymer 47 (2006) 1108-1118

[35] Jasso, C. F., Jesus Martinez, J., Mendizabal, E., Laguna, O., *Mechanical and rheological properties of styrene/acrylic gradient polymers*, Journal of Applied Polymer Science 58 (1995) 2207-2212

[36] Dhoke, S. K., Palraj, S., Maruthan, K., Selvaraj, M., *Preparation and characterization of heat-resistant interpenetrating polymer network (IPN)*, Progress in Organic Coatings 59 (2007) 21-27

[37] Meseguer Dueñas, J. M., Torres Escuriola, D., Gallego Ferrer, G., Monleón Pradas, M., Gómez Ribelles, J. L., Pissis, P., Kyritsis, A., *Miscibility of Poly(butyl acrylate)-Poly(butyl methacrylate) Sequential Interpenetrating Polymer Networks*, Macromolecules 34 (2001) 5525-5534